

# Dissolved methane concentrations and fluxes to the atmosphere from a tropical floodplain lake

Pedro M. Barbosa : John M. Melack · João H. F. Amaral · Sally MacIntyre · Daniele Kasper · Alicia Cortés · Vinicius F. Farjalla · Bruce R. Forsberg

Received: 2 June 2019/Revised: 4 February 2020/Accepted: 19 February 2020/Published online: 2 March 2020 © Springer Nature Switzerland AG 2020

**Abstract** Large uncertainties in estimates of methane (CH<sub>4</sub>) emissions from tropical inland waters reflect the paucity of information at appropriate temporal and spatial scales. CH<sub>4</sub> concentrations, diffusive and ebullitive fluxes, and environmental parameters in contrasting aquatic habitats of Lake Janauacá, an Amazon floodplain lake, measured for two years revealed patterns in temporal and spatial variability related to different aquatic habitats and environmental conditions. CH<sub>4</sub> concentrations ranged from below detection to 96  $\mu$ M, CH<sub>4</sub> diffusive fluxes from below detection to 2342  $\mu$ mol m<sup>-2</sup> h<sup>-1</sup>, and CH<sub>4</sub> ebullitive fluxes from 0 to 190 mmol m<sup>-2</sup> d<sup>-1</sup>. Vegetated aquatic habitats had higher surface CH<sub>4</sub> concentrations than open water habitats, and no

significant differences in diffusive CH<sub>4</sub> fluxes, likely due to higher *k* values measured in open water habitats. CH<sub>4</sub> emissions were enhanced after a prolonged low water period, when the exposed sediments were colonized by herbaceous plants that decomposed after water levels rose, possibly fueling CH<sub>4</sub> production. Statistical models indicated the importance of variables related to CH<sub>4</sub> production (temperature, dissolved organic carbon) and consumption (dissolved nitrogen, oxygenated water column), as well as maximum depth, in controlling surface water CH<sub>4</sub> concentrations.

**Keywords** Amazon floodplain  $\cdot$  CH<sub>4</sub> emission  $\cdot$  Carbon cycle  $\cdot$  Wetlands

Responsible Editor: Breck Bowden

**Electronic supplementary material** The online version of this article (doi:https://doi.org/10.1007/s10533-020-00650-1) contains supplementary material, which is available to authorized users.

P. M. Barbosa (☒) · D. Kasper · V. F. Farjalla Departamento de Ecologia, Instituto de Biologia, Universidade Federal do Rio de Janeiro, Rio de Janeiro, Rio de Janeiro, Brazil e-mail: pebarbosa.limno@gmail.com

P. M. Barbosa · J. M. Melack · J. H. F. Amaral · S. MacIntyre · A. Cortés Earth Research Institute, University of California, Santa Barbara, CA, USA J. H. F. Amaral · B. R. Forsberg Coordenação de Dinâmica Ambiental, Instituto Nacional de Pesquisas da Amazônia, Manaus, Amazonas, Brazil

D. Kasper Instituto de Biofísica Carlos Chagas Filho, Universidade Federal do Rio de Janeiro, Rio de Janeiro, Brazil

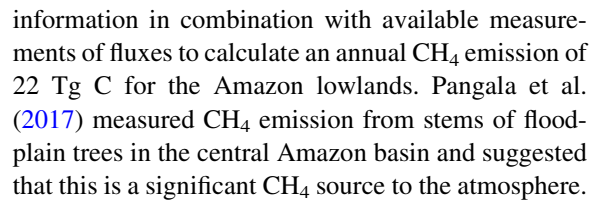


## Introduction

Methane (CH<sub>4</sub>) concentrations have almost doubled in the global atmosphere over the last 150 years (Wang et al. 2014), and methane is now the second most important climate-forcing gas (Saunois et al. 2016). Recent estimates of global emissions indicate that 596 to 884 Tg  $CH_4$  is emitted to the atmosphere each year, and this flux is being increased by human activities (Saunois et al. 2016). Wetlands and inland waters are the single largest natural source of atmospheric  $CH_4$  (Kirschke et al. 2013).

Wetlands cover extensive areas in high latitudes and in tropical regions (Kirschke et al. 2013). Riverine floodplains constitute the largest wetland areas in the tropics and are characterized by seasonal floods that promote the exchange of nutrients and organisms among habitats and substantial primary production (Junk 1997). Due to these factors, together with high temperatures, tropical wetlands are thought to be responsible for the majority of global wetland CH<sub>4</sub> emissions (Bloom et al. 2012; Bridgham et al. 2013; Melton et al. 2013). However, large uncertainties persist in estimates of tropical CH<sub>4</sub> emission, largely due to the paucity of studies at appropriate temporal and spatial scales and the few sites with measurements.

Amazon floodplains and wetlands cover an area of approximately 1 million km<sup>2</sup>, and include open water environments (lakes and river channels), seasonally flooded forests and areas dominated by emergent and floating herbaceous plants (Hess et al. 2015; Junk et al. 2011; Melack and Forsberg 2001). Due to the heterogeneity of the floodplains and their complex hydrology, considerable spatial and temporal variability in CH<sub>4</sub> concentrations and fluxes to the atmosphere have been reported based on short-term studies at specific sites or occasional regional surveys. Bartlett et al. (1988) and Devol et al. (1988) reported higher fluxes in vegetated habitats than in open waters. Devol et al. (1990) and Barbosa et al. (2016) provided evidence of seasonal variations in fluxes from lakes and rivers. Estimates of the contribution of different emission pathways of CH<sub>4</sub> evasion suggested a higher contribution from ebullition than other pathways (Bartlett et al. 1988; Crill et al. 1988; Wassmann et al. 1992). Melack et al. (2004) were the first to use regional analyses of microwave remote sensing data to establish inundated areas and habitats, and used that



Methane emission to the atmosphere from aquatic environments reflects differences between CH<sub>4</sub> production, mainly in anoxic sediments, and consumption by methanotrophs (Bastviken 2009; Thottathil et al. 2019), as well as effects of water movements and mixing (MacIntyre and Melack 1995). These processes are influenced by environmental variables such as water temperature, dissolved oxygen and substrate availability for methanogens and methanotrophs. Ebullitive fluxes depend on bubble formation and hydrostatic pressure over the sediment (Bastviken 2009), while diffusive fluxes are dependent on concentration gradients aided by turbulent mixing, which vary on multiple time and space scales (Poindexter et al. 2016; Yun et al. 2013). Factors such as wind speed, diel variation in thermal structure and physical processes such as convective and advective mixing are all known to influence gas distributions and transfer velocities, and consequently gas fluxes, but have received little attention in tropical floodplains (MacIntyre and Melack 1995; MacIntyre et al. 2010; MacIntyre et al. 2019; Tedford et al. 2014).

The majority of studies done in the Amazon basin have entailed infrequent sampling primarily in open waters of lakes or rivers (Bartlett et al. 1988; Crill et al. 1988; Devol et al. 1988, 1990). Few studies have covered a complete hydrological cycle (Wassmann et al. 1992; Barbosa et al. 2016), and rarely were diel variation in CH<sub>4</sub> dynamics considered. Limnological, hydrological and meteorological data have rarely been measured together with gas measurements, limiting the assessment of the influence of ecological factors, thermal structure and other processes on CH<sub>4</sub> fluxes and concentrations. Ebullitive fluxes have been estimated only using floating chambers with short-time deployments.

The present study was designed with two main objectives: (i) to measure CH<sub>4</sub> concentrations and fluxes (diffusive and ebullitive) at diel, seasonal and interannual time scales, in three common habitats (open water, floating herbaceous plants and flooded forest) of the Amazon white-water river floodplains, known as *várzea*; and (ii) to identify environmental



conditions that explain differences in  $CH_4$  concentrations in and among these habitats. This is the first study to combine high-resolution measurements of  $CH_4$  fluxes with auxiliary limnological and meteorological data in these habitats over multiple time scales. By sampling during two consecutive hydrological years we evaluated interannual differences and the consequences of an exceptional variation in inundation. In addition, we calculated gas transfer velocities ( $k_{617}$ ) under a variety of conditions and measured directly ebullitive flux.

Our results contribute to understanding of the complex CH<sub>4</sub> dynamics in tropical floodplain environments and address several questions: (i) How do environmental conditions during different hydrological phases influence methane concentrations and fluxes? (ii) How do CH<sub>4</sub> concentrations and fluxes to the atmosphere vary between day and night? (iii) Are fluxes higher in or near vegetated areas than in open waters? (iv) How do extended periods of low water with associated growth and inundation of plants alter methane concentrations?

## Material and methods

# Study area and sampling

The study was conducted in a large floodplain lake (Lake Janauacá) on the southern margin of the Solimões River, 40 km southeast of Manaus, Brazil (3° 23′ S; 60° 18′ W; Fig. 1). It has a local watershed area of 770 km<sup>2</sup> and a floodable area that varies from 23 to 390 km<sup>2</sup> between the low and high water periods, respectively (Pinel et al. 2015). Due to the seasonal variation of rainfall in the upper Amazon basin, the Solimões River has a large oscillation in water level  $(\sim 10 \,\mathrm{m})$  (Paiva et al. 2013) causing seasonal changes in lake depth from 0 to 3 m during the low water period, and from 9 to 13 m during the higher water period. The lake is permanently connected to the Solimões River by a channel. The northern part of the lake, where our sampling sites are located, is a floodplain with a mixture of upland and Solimões River water (Bonnet et al. 2017). As in other Amazon lakes, the distribution of aquatic habitats varies in L. Janauacá, depending on the hydrological phase. During the low water period, only open water habitats occur, while during the rising and high water periods, extensive flooded forest and floating herbaceous macrophytes are present.

Sampling was done at two sites; location of each site changed slightly depending on water level. One site, called embayment (3.40619° S, 60.24627° W) is in a small bay surrounded by seasonally inundated trees about 20 m high and with a fetch of 50 to 100 m for most common wind directions. The other site, called open lake (3.37985° S, 60.25397° W) is located in or adjacent to a large open water area, and had a fetch varying from 1 to 4 km depending on wind direction and water level. Within each site, we sampled in three habitats: open water, floating herbaceous plants (referred to as macrophyte mats), and flooded forests. Amaral et al. (2020) provides highresolution images of the two sites with the embayment called wind protected and the open lake called wind exposed. We sampled on 19 occasions between August 2014 and September 2016 (Fig. 2). Each sampling campaign was approximately 8 days. Year 1 was from August 2014 to August 2015, and year 2 was from September 2015 to September 2016. The second year had exceptionally low water levels from October to February, with large areas of lake bottom exposed and colonized by herbaceous vegetation.

#### Environmental variables

Sampling started in the morning ( $\sim 6$  a.m.), and was done in all habitats, whenever they were present (Fig. 2). Each site and habitat was sampled at least three times over a period of 24 h, depending on depth of the water column and habitat availability. During each sampling, measurements of CH<sub>4</sub> concentrations and fluxes, and temperature, dissolved oxygen (DO) and conductivity profiles were done. Temperature and DO concentrations were measured with a temperature/ oxygen meter (Yellow Springs Inst. Co., model ProODO, accuracy of  $0.2 \pm 0.1$  mg L<sup>-1</sup>, temperature accuracy  $\pm$  0.2 °C, resolution 0.1 °C) at 0.5 m intervals from the surface to the bottom of the lake. We used the manual profiles of DO to estimate the oxygenated part of the water column (Z\_oxy), the depth with DO at or above  $0.4 \text{ mg L}^{-1}$ . Conductivity was measured using a profiler (resolution 1  $\mu$ S cm<sup>-1</sup>; Castway, Sontek Inst. Co.), sampling at 4 Hz, with data reported at 0.3 m intervals. pH was measured at depths of 0.3 m, mid water, and 0.5 m from sediment with a portable pH meter (Orion Star, Thermo



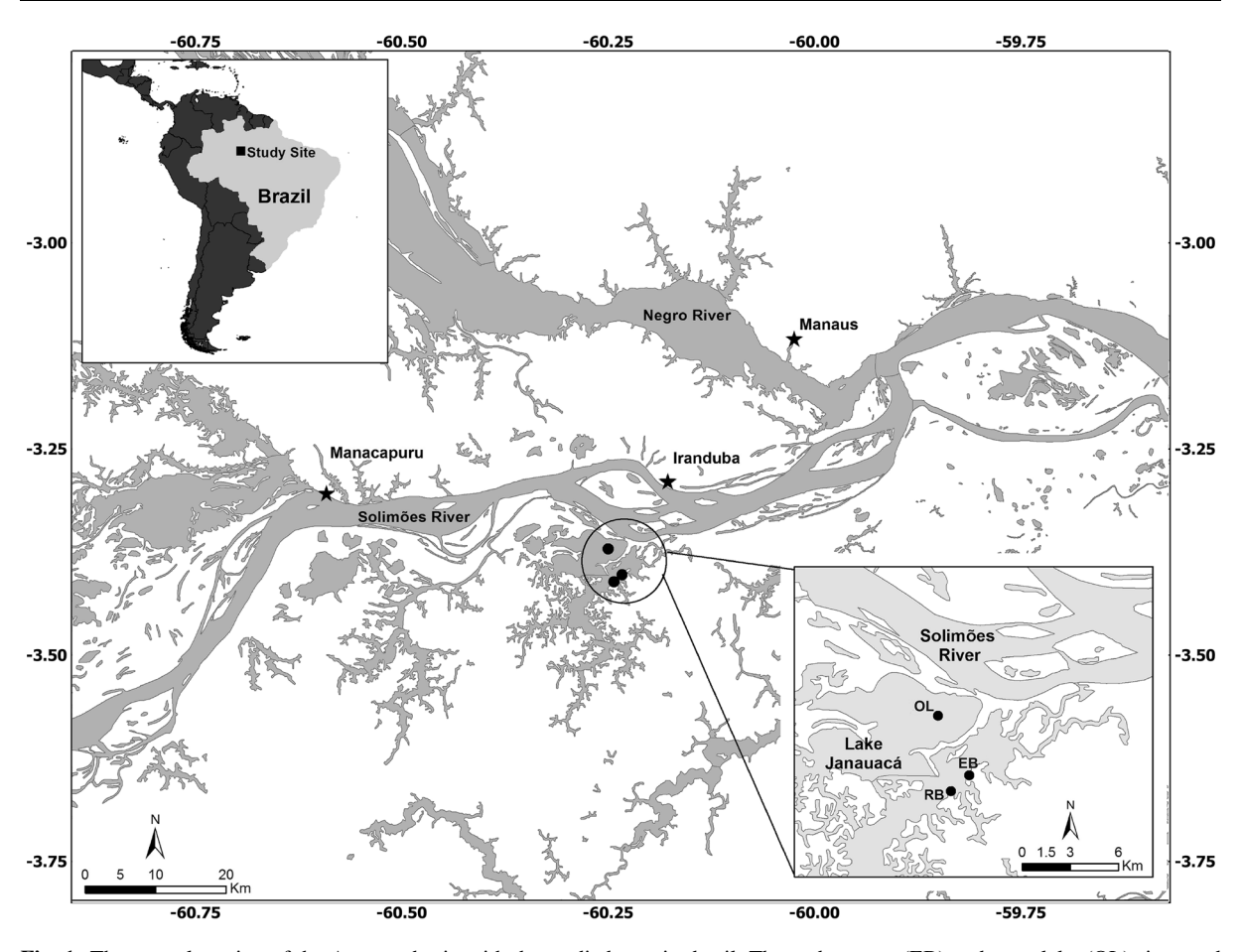


Fig. 1 The central portion of the Amazon basin with the studied area in detail. The embayment (EB) and open lake (OL) sites, and research base (RB) are marked with black dots

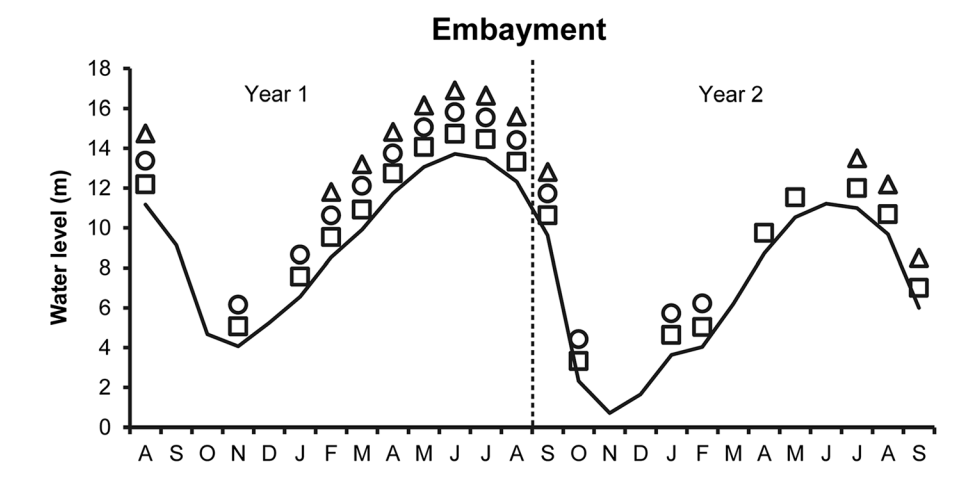
Scientific; precision 0.1), using a peristaltic pump to obtain water from lower depths. A floating buoy with wind speed and direction sensors (Onset, Inc.) at 2 m height was deployed close to where  $\mathrm{CH_4}$  measurements were made at both open water sites.

Time series measurements of temperature and dissolved oxygen were obtained from multiple sensors on taut-line moorings. The number of sensors varied with water level, and deployment depths were chosen based on manual profiles of temperature and dissolved oxygen. Due to the short deployment periods (no more than 5 days at each site), sensors did not require protection from biofouling. The temperature sensors were RBR Solos with 0.002 °C accuracy and 0.05 °C resolution recording every 10 s. Dissolved oxygen was measured with optical sensors (PME MiniDOT loggers) recording every 10 min (accuracy of 5% of

measurement or  $0.3 \text{ mg L}^{-1}$ , whichever is larger, and resolution of  $0.01 \text{ mg L}^{-1}$ ).

We sampled water for chlorophyll-a (chl-a), dissolved organic carbon (DOC), total suspended solids (TSS), total nitrogen (TN) and total phosphorous (TP) analyses from the three habitats at both sampling sites. Sampling was made at 0.5 m, and water was stored in insulated boxes until processing. For chl-a analyses, water was filtered through glass fiber GF/F filters (Whatman). Filters were maintained frozen and in the dark until analysis. Chl-a was determined spectrophotometrically, following filter maceration and extraction in 90% acetone, using trichromatic equations (Strickland and Parsons 1972). TSS was determined by weighing particulates collected on pre-weighed Millipore HA filters (0.45 µm pore size), following Kasper et al. (2018). DOC samples were filtered through pre-combusted (450-500 °C for 1 h) glass





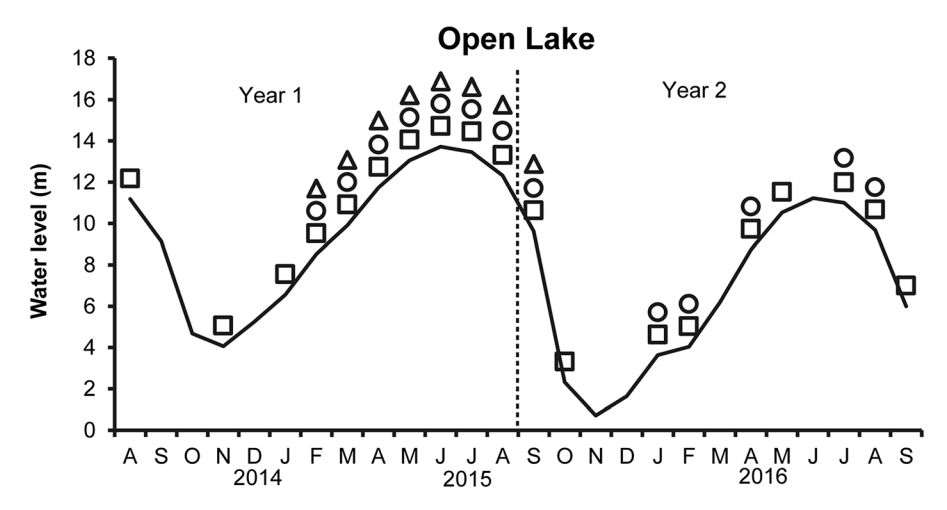


**Fig. 2** Water level at Lake Janauacá (continuous line). Sampling campaigns from August 2014 to September 2016 are marked each month for the sampled aquatic habitats: open water (open squares), macrophyte mats (open circles), and flooded forest (open triangles), in the embayment (upper panel), and open lake sites (lower panel). Dashed lines separate hydrological years. Year 1 included low water (November

2014), rising water (January, February, March, and April 2015), high water (May, June, and July 2015, July 2015), and falling water (August 2014 and 2015). Year 2 included low water (October 2015), rising water (January, February, and April 2016), high (July and August 2016), and falling water (September 2016)

fiber GF/F filters (Whatman), collected in pre-cleaned (10% HCl wash, deionized water rinse) and pre-combusted (450–500 °C for 1 h) borosilicate vials and then stored at 4 °C until analysis. DOC was determined using a total organic carbon analyzer (TOC-V Shimadzu). TN and TP were determined by simultaneous analysis on unfiltered samples after persulfate digestion (Valderrama 1981) and nitrate and phosphorus assays (Strickland and Parsons 1972). Vertical profiles of photosynthetically available radiation (PAR) were determined using an underwater sensor (Licor LI-192 SB), and downwelling attenuation was

calculated from the slope of a linear regression between the Ln (PAR) and depth. Water transparency was estimated with a Secchi disk.

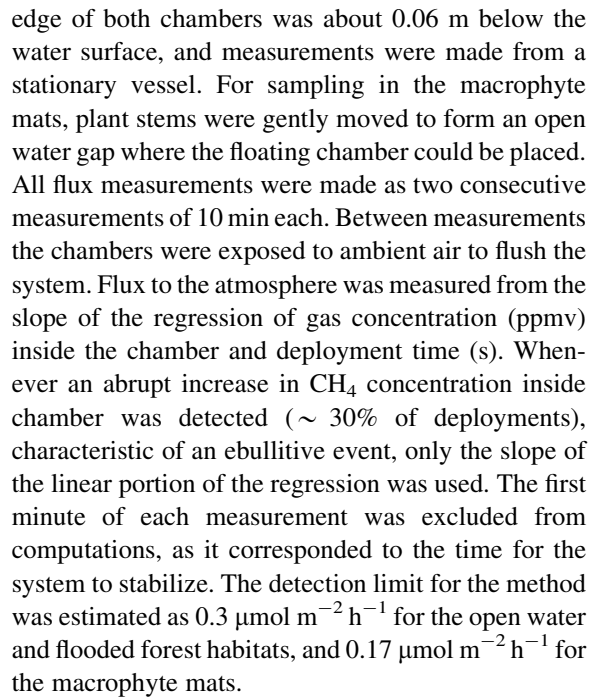
Water levels were manually read daily in both years from stage gauges installed at two locations with associated altimetry (Bonnet et al. 2017). These daily measurements were used to estimate  $\triangle Z$ , which was the water level change over the 10 days before each sampling period.



## Dissolved CH<sub>4</sub> concentrations and fluxes

Water for determination of dissolved CH<sub>4</sub> concentrations ([CH<sub>4</sub>]) was sampled at 0.2 m below the surface, depth of the oxycline (defined using the DO profiles), and 0.5 m from the bottom, at least three times a day (early morning, noon, night) at each sampling site, with the exception of May 2016, when only afternoon sampling was done. Water samples for determination of [CH<sub>4</sub>] from the sub-surface were collected with 60 mL polyethylene syringes, and a peristaltic pump was used for oxycline and near-bottom sampling. Gas samples for CH<sub>4</sub> analyses were obtained using a headspace technique by vigorous shaking of equal volumes (30 mL) of water and air in the sampling syringe for 2 min (Hamilton et al. 1995). Using two syringe needles, the equilibrated air was then transferred to 20 mL glass serum vials, previously cleaned with HCl (10%) and rinsed with deionized water and filled with distilled water saturated with salt. Samples were stored at room temperature in the dark until analysis. Analyses were performed no longer than 15 days after sampling using a gas chromatograph (Thermo Scientific), equipped with a flame ionization detector. Calibration was done using gas standards of 10 ppmv and 100 ppmv CH<sub>4</sub> (Air Liquide, USA), and the equipment was recalibrated after every 25 to 30 samples. The detection limit was approximately 0.004 μM. The solubility coefficients in Yamamoto et al. (1976) were used to estimate [CH<sub>4</sub>]. As atmospheric air was used for equilibration, the atmospheric CH<sub>4</sub> concentration was included in the calculation (for more datails about the procedures, see Barbosa et al. 2016).

Diffusive CH<sub>4</sub> fluxes to the atmosphere were measured using floating chambers, connected to an off-axis integrated cavity output spectrometer (Ultraportable Greenhouse Gas Analyzer—UGGA, Los Gatos Research). Air circulated in the system (chamber and UGGA) in a closed circuit, with CH<sub>4</sub> concentrations inside the chamber measured every 10 s for a deployment time of 10 min. The chamber used in the open water and flooded forest habitats had an internal volume of 15 L and an internal area of 0.11 m<sup>2</sup>, and the chambers used in the macrophyte mats had an internal volume of 5 L and an internal area of 0.06 m<sup>2</sup>. To permit equilibration with the inside and outside pressures a 2 mm diameter (3 m long) polyethylene tube was inserted into the top of the chambers. The



In a few cases (n = 14, or 1.7%), high wind speeds resulted in unrealistic diffusive fluxes, so we choose to estimate those using the gas transfer velocities (k) estimated after Tedford et al. (2014) and [CH<sub>4</sub>] in the surface. MacIntyre et al. (2019) shows that calculated k values based on a surface renewal model and k values calculated from chamber measurements for Amazon floodplain habitats are within the inherent variability of gas transfer velocities. On a few other occasions (n = 14, or 1.7%), when we could not measure an exclusively diffusive flux due to persistent capture of bubbles in the chambers, k estimated from CO<sub>2</sub> fluxes was used to estimate CH<sub>4</sub> fluxes.

Gas transfer velocities were estimated using diffusive flux measurements made with floating chambers and solving the following equation for *k*:

$$F = k(C_{\rm w} - C_{\rm eq})$$

where F is the CH<sub>4</sub> diffusive flux (mmol m<sup>-2</sup> h<sup>-1</sup>), k is the gas transfer velocity (m h<sup>-1</sup>), C<sub>w</sub> is the observed dissolved CH<sub>4</sub> concentration and C<sub>eq</sub> is the CH<sub>4</sub> concentration in equilibrium with the atmosphere. The estimated k values were temperature normalized to a Schmidt (Sc) number of 617 (k<sub>617</sub>) using the equation:



$$k\text{CH}_4 = k \left(\frac{617}{Sc}\right) - 0.5$$

where Sc is the Schmidt number for water temperature T (°C) calculated following Wanninkhof (2014):

$$Sc = 1909.4 - 120.78T + 4.1555T2 - 0.080578T3 + 10.00065777T4$$

# Ebullitive CH<sub>4</sub> flux

Estimates of ebullitive flux were made with inverted funnels (each 0.3 m diameter; six to nine funnels per measurement period). A polyethylene bottle (0.3 L volume) filled with water was connected to each funnel; as gas bubbles were captured by the funnel, the water was expelled from the bottled. The funnels were placed in both open water and flooded forest (whenever possible) habitats, in the embayment and open lake sites, and were deployed for at least 24 h. Gas samples were taken using plastic syringes and transferred to 20 mL glass serum vials filled with distilled water saturated with salt, as described above.

Ebullitve flux was calculated according to the following equation:

$$FCH_4eb = \frac{[CH_4] \times CH_4Vol}{A \times td}$$

where FCH<sub>4</sub>eb is the ebullitive flux (mmol m<sup>-2</sup> d<sup>-1</sup>), [CH<sub>4</sub>] is the dissolved CH<sub>4</sub> concentration (mmol m<sup>-3</sup>); CH<sub>4</sub> Vol is the gas volume sampled (m<sup>3</sup>); A is the funnel area (m<sup>2</sup>); and td is deployment time (days). A graduated 60 mL syringe with a three-way valve was used to extract and measure the volume of gas captured by each funnel. All samples for CH<sub>4</sub> concentration were analyzed with a gas chromatographer equipped with a flame ionization detector. Due to problems with deployment of bubble traps, ebullitive flux could not be measured during in February and March 2015, and April, May, July and August 2016.

## Statistical analyses

Normality tests indicated that  $CH_4$  surface concentrations, fluxes to the atmosphere and  $k_{617}$  had a normal distribution after being log-10 transformed, while bottom  $CH_4$  concentrations remained non-normal. Due to the extended low water period in year 2,

seasonal comparisons were made using only data from year 1 and interannual comparisons were only possible for open water habitats because of limited access to other habitats. Interannual analyses were done using two-way ANOVA followed by Tukey post-tests for the normal distributed variables, and Kruskal-Wallis tests for the non-normal distributed variable. For seasonal analyzes, ANOVA were used, followed by Tukey post-test, and Kruskal-Wallis tests. We use paired t-tests to compare day (6 a.m.-6 p.m.) versus night (6 p.m.-6 a.m.) values of diffusive fluxes, surface concentrations, and  $k_{617}$  for all habitats. Spatial comparisons of surface and bottom [CH<sub>4</sub>]s, diffusive fluxes and  $k_{617}$  between habitats of the embayment and open lake sites were done using t-tests. Graphs and statistical analyzes were done using in R (R Core Development Team 2018).

In order to identify possible environmental variables that could explain seasonal variation of surface [CH<sub>4</sub>], and to check for collinearity among those variables, we first performed a principal component analysis (PCA) with all the sampled variables with possible influence on [CH<sub>4</sub>]. As some of these environmental variables were sampled only once a day, while others were sampled every time a flux measurement was made, we used daily averages (whenever possible) of the environmental variables in the PCA and models. The PCA function from the vegan package (Oksanen et al. 2018) in R (R Core Development Team 2018) was used. We then used linear mixed-effects models to determine a set of plausible models according to an information theoretic approach (Gruner et al. 2017). We first fitted a linear mixed-effects model (GLMM) for each habitat (open water, flooded forest and macrophyte mats) pooling the embayment and open lake data together, using the *lmer* function implemented in the *lme4* package in R (Bates et al. 2017). Prior to generating the models, we used the variance inflation factor (VIF) analysis to identify which independent variables were collinear, and a threshold of 5 was chosen to remove collinear variables. We also used the r.squaredGLMM function in R to generate a R<sup>2</sup> value for each model. As suggested by Nakagawa and Schielzeth (2013), we chose to present the marginal and conditional R<sup>2</sup>, as the former provides the variance explained by the fixed factors alone, while the latter is related to the variance of both fixed as well as random factors. Once we established this model, we standardized the



response and all predictor variables using the *arm* package (Gelman and Su 2018), a step for interpreting the parameter estimates after model averaging. From this model we generated a confidence set, using the *dredge* function available in the *MuMIn* package (Barto'n 2018). We used the function *get.models* from the *MuMIn* package to obtain the top models within two units of  $\Delta$ AICc of the 'best' model (Grueber et al. 2011). As a final step we used the *model.avg* function in R to estimate parameter coefficients in the confidence set, calculating conditional values using the mean of regression coefficients weighted by the AIC weight ( $w_i$ ) from each model including that variable (Gruner et al. 2017).

#### Results

## Methane and environmental conditions

CH<sub>4</sub> concentrations and fluxes varied temporally and spatially. Temporally, values varied during hydrological phases, different years, as well as over 24 h periods, and spatially, within and between sites (Table 1). We present data as ranges and geometric means (GM) for concentrations and diffusive fluxes and ranges and medians for ebullitive fluxes. Surface [CH<sub>4</sub>] varied from below detection to 95.6 μM (n = 818; GM = 0.8  $\mu$ M), and dissolved [CH<sub>4</sub>] in bottom waters ranged from 0.04 µM to 468 µM (n = 399; GM = 4.2  $\mu$ M). Diffusive fluxes varied from below detection to 2,342 µmol m<sup>-2</sup> h<sup>-1</sup> (n = 845: GM = 16.9  $\mu$ mol m<sup>-2</sup> h<sup>-1</sup>), and ebullitive fluxes varied from 0 to 109 mmol  $m^{-2} d^{-1}$  (n = 225; median =  $2 \text{ mmol m}^{-2} \text{ d}^{-1}$ ) (Table 1). These concentrations and fluxes were highly right skewed (Fig. S1).  $k_{617}$  values for all habitats and periods ranged from negligible to 23 cm h<sup>-1</sup> (Table 1). Surface [CH<sub>4</sub>] and fluxes were higher during lower water, while bottom [CH<sub>4</sub>] was higher during high water periods. Fluxes from the habitats in the embayment were significantly higher than those from habitats at the open lake site (Mann–Whitney test,  $p \le 0.0001$ ).

Environmental conditions in the sampled habitats changed with water level. During low and rising water periods, chl-a, DO, TN and TSS were higher than during high water periods (Tables S1 and S2). The lower conductivities during low water reflects runoff

from local streams. More information about environmental conditions at each site is provided in Supplemental Materials. Habitats in the embayment developed vertical temperature and oxygen gradients at the beginning of the rising water period. During high water, DO above  $\sim 0.5 \text{ mg L}^{-1}$  was present to only about 2 m (e.g., Fig. 3). This coincides with the period of higher bottom [CH<sub>4</sub>], but lower fluxes and surface [CH<sub>4</sub>]. At the open lake site, shallow diurnal thermoclines formed during the morning, deepened with changes in wind velocity and solar inputs, and the water column mixed and was oxygenated at night for most of the year with the exception of the high water period and occasionally on sunny days (e.g., Fig. 4). Wind speeds in the embayment site were usually below detection ( $< 0.4 \text{ m s}^{-1}$ ), and rarely exceeded 2.5 m s<sup>-1</sup>, with the exception of rainstorms, when speeds briefly rose to 5 m s<sup>-1</sup>. Wind speeds tended to be higher in early afternoon and lower at night and early morning. At the open lake site, wind speeds were generally between 2.5 and 5 m s<sup>-1</sup>, with values up to 10 m s<sup>-1</sup> during some storm events and were higher in the afternoon and lower at night. These differences in stratification and mixing patterns between the two sites led to large differences in surface and bottom [CH<sub>4</sub>] between sites. Values were up to 6 and 30 times higher for surface and bottom concentrations in the open water habitat of the embayment site than at open lake site (GM = 1.2  $\mu$ M and 18.3  $\mu$ M, and GM = 0.2 μM and 0.6 μM for surface and bottom [CH<sub>4</sub>] of the embayment and open lake sites, respectively).

## Within habitat temporal differences

Surface [CH<sub>4</sub>]: In open water of the embayment site, surface [CH<sub>4</sub>] during rising water were significantly lower than those measured during low (Tukey posttest, p = 0.007) and falling waters (Tukey posttest, p = 0.004; Fig. 5a; Table 1). Higher surface [CH<sub>4</sub>] when water levels were lower was observed at the open lake site, where surface [CH<sub>4</sub>] was higher during falling water (Tukey post-test, p = 0.0006, p = 0.003, p < 0.0001 for high, low, and rising water, respectively) (Figs. 5c). In the macrophyte mats, no significant seasonal differences in surface [CH<sub>4</sub>] were found (ANOVA, f = 2.69, p = 0.06) for the embayment site, while at the open lake site higher values occurred during falling water compared to other periods (high water, Tukey post-test, p = 0.0005, and rising water,



**Table 1** Dissolved CH<sub>4</sub> surface and bottom concentrations, diffusive (FCH<sub>4</sub>diff) and ebullitve (FCH<sub>4</sub>eb) fluxes to the atmosphere and gas transfer coefficients ( $k_{6/7}$ ) for the three aquatic habitats (open water, macrophyte mat, flooded forest) sampled at each site (embayment and open lake), for the hydrological periods of low (LW), rising (RW), high (HW),

	Open water	L			Macrophyte				Flooded forest	rest	
	ΓM	RW	HW	FW	LW	RW	HW	FW	RW	HW	FW
Embayment											
$CH_4$ surf. ( $\mu M$ )	0.5–7.7	0.04 - 9.2	0.2-15.5	0.2 - 11.2	0.3-95.7	0.3-47.3	1.2–36.1	0.4–27.7	0.07-0.8	0.2 - 3.1	0.6 - 10.8
	(2.2)	(1.1)	(1.0)	(1.1)	(5.1)	(2.2)	(3.9)	(3.5)	(0.3)	(0.7)	(1.6)
CH <sub>4</sub> Bott. (µM)	0.5–7.7	0.1–372	0.06 - 306	0.7-468	1–111	0.1 - 121	14.7–127.8	11.2–121	0.07 - 2.4	1.8–92	1.2–54
	(2.4)	(15)	(94)	(18)	(11)	(6.3)	(76.3)	(51.4)	(0.6)	(24.7)	(7.3)
$FCH_4$ dif (µmol m <sup>-2</sup> h <sup>-1</sup> )	15.4–564	3–688	2.8-1399	9.7–213	2.6-2342	3.7–75.2	3.7–71.4	2–26.5	2.5–38	2.3–25	8.8–99
	(117)	(40)	(16.3)	(46.5)	(134)	(19)	(15.6)	(6.3)	(9.2)	(9.9)	(25.6)
$FCH_4eb \text{ (mmol m}^{-2} d^{-1})$	0-51.3	0-4.2	0-5.3	0-3.2	na	na	na	na	0.5-5.4	0.01 - 12.5	0.01 - 18.6
	(22.1)	(1.6)	(2.4)	(1.6)					(2.5)	(3.2)	(4.5)
$k_{617}  (\text{cm h}^{-1})$	1–11	0.3-14	0.4–7	0.5-13	0.1–14	0.1-4	0.01-3	0.01 - 0.6	0.3-5	0.2-4	0.1–5
	(4)	(3)	(1.4)	(3.4)	(2)	(0.75)	(0.3)	(0.2)	(1.5)	(0.7)	(1.2)
Open lake											
CH <sub>4</sub> surf. (µM)	0.1-0.8	0.01 - 2.1	-BD - 6.4	0.1 - 3.2	na	0.05-56	0.06-4.4	0.07-9.0	0.02 - 0.5	0.05 - 0.6	0.3-5.5
	(0.3)	(0.2)	(0.2)	(0.2)		(1.8)	(0.3)	(1.1)	(0.1)	(0.2)	(1.7)
CH <sub>4</sub> Bott. (µM)	0.1 - 4.6	0.06 - 2.5	0.04-9.3	0.1 - 95.7	na	0.12 - 70	0.1–299	0.2–21.5	0.1-1.0	0.2-2.2	0.3-24.6
	(0.4)	(0.6)	(0.5)	(1.3)		(4.8)	(4.5)	(2.2)	(0.3)	(0.5)	(2.2)
$FCH_4dif (\mu mol m^{-2} h^{-1})$	4.8-98.9	0.4–249	BD-93.1	0.66 - 134	na	2.6-834	0.3–23.2	1.3–34.7	0.4–646	BD-9.5	2-137.2
	(23)	(12.4)	(2.5)	(10.9)		(40.5)	(2.9)	(6.8)	(14.3)	(1.8)	(23.1)
$FCH_4eb \text{ (mmol m}^{-2} d^{-1})$	0-12.8	0-0.2	0-0.02	0.02-2.5	na	na	na	na	0-0.04	0-1.2	0-109
	(7.1)	(0.02)	(0.01)	(0.4)					(0.02)	(0.14)	(0.3)
$k_{617} \; (\mathrm{cm} \; \mathrm{h}^{-1})$	4-17	0.5-18	0.03-14.7	0.1 - 22.7	na	0.2-17	0.02-16	0.2-5	3–13	0.2–5	0.1–6.2
	(7)	(3.8)	(1.4)	(4)		(1.4)	(0.7)	(0.74)	(5)	(1.3)	(1)

na not available



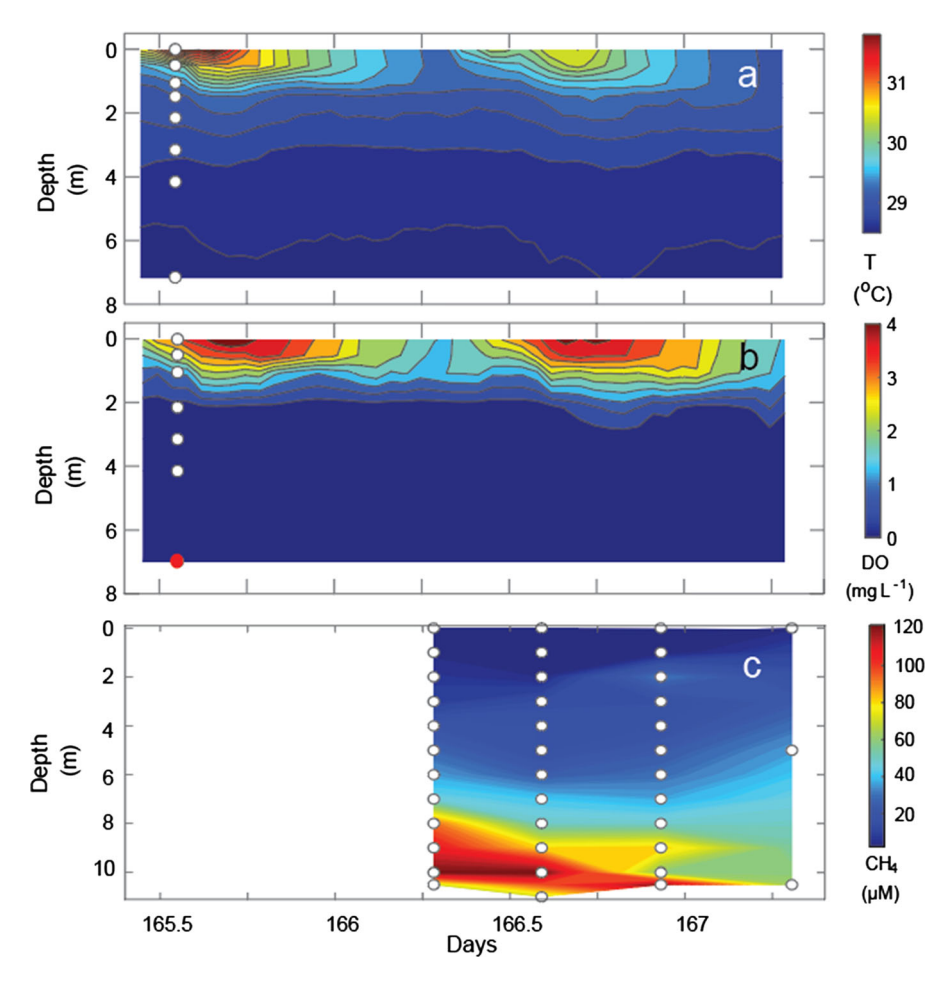


**Fig. 3** Hourly-averaged time-depth diagrams of water temperature (T) with isotherms every 0.2 °C (a), and dissolved oxygen (DO) with oxygen isopleths every 0.4 mg  $L^{-1}$  (b), and  $CH_4$  concentrations (c) measured in the open water habitat in the

embayment during the period 14 to 16 June 2015 for **a**, **b**, and during the period 15 to 16 June 2015 for **c**. White dots are the depth of the sensors. The red dot marks DO from manual profiles. Diurnal heating and nocturnal cooling are evident

Tukey post-test, p = 0.006). In the flooded forest habitat, higher surface [CH<sub>4</sub>] was measured during falling water at both sampled sites: open lake (high, Tukey post-test, p < 0.0001, and rising Tukey post-test, p < 0.0001 periods), and embayment (high - Tukey post-test, p = 0.028, and rising water Tukey post-test, p = 0.0006 periods).

 $CH_4$  diffusive fluxes At both sites, higher diffusive fluxes were associated with lower water levels. In open water at the embayment site, higher fluxes occurred during the low water period when compared to high (Tukey post-test, p = 0.007), and rising (Tukey post-test, p = 0.009) water periods (Figs. 5b; Table 1). Similarly, fluxes during high water were significantly lower than those during low (Tukey post-test,

p = 0.002; Figs. 5d) and falling water (Tukey posttest, p = 0.003) at the open lake site. In the macrophyte mats at the embayment site, diffusive fluxes measured during falling water were significantly lower than those measured in high (Tukey post-test, p = 0.04) and rising (Tukey post-test, p = 0.009) water periods (Fig. S2a), contrasting with the results for the open lake site, where high water fluxes were significantly lower than the falling (Tukey post-test, p = 0.035), and rising water ones (Tukey post-test, p = 0.002; Fig. S3a). In the flooded forest habitats, fluxes during falling water were higher than those measured during high and rising water periods for both sites (ANOVA, p < 0.05; Figs. 2b, 3b).



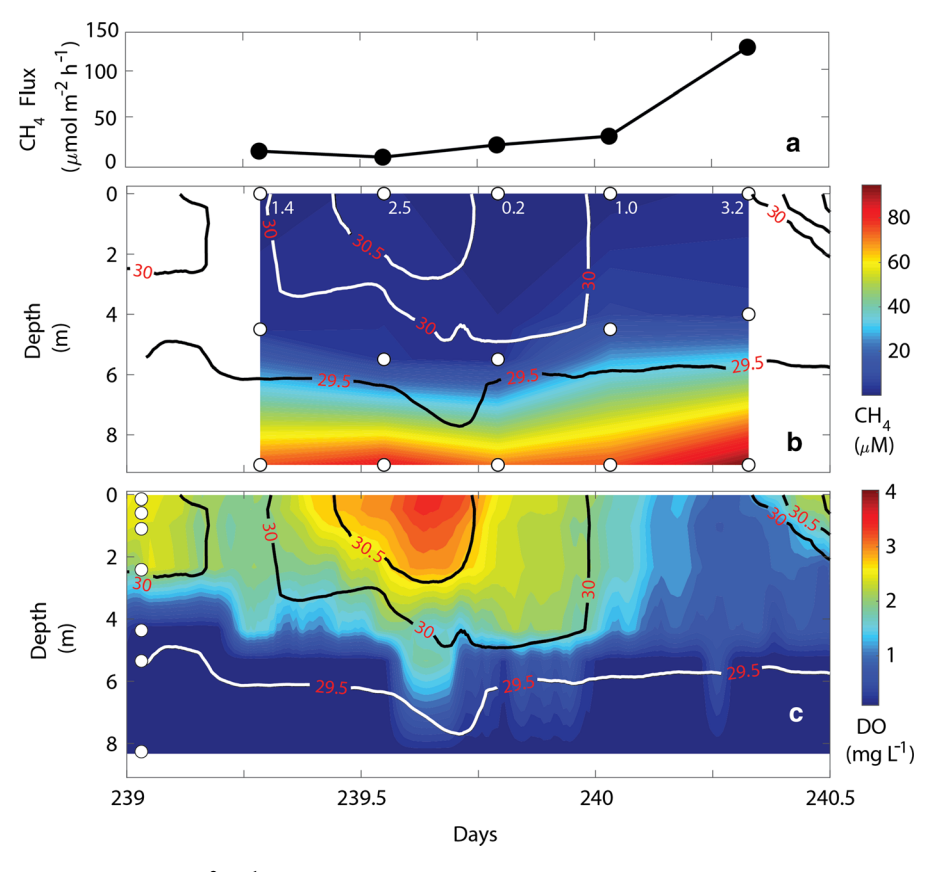


**Fig. 4** CH<sub>4</sub> diffusive flux ( $\mu$ mol m<sup>-2</sup> h<sup>-1</sup>) (**a**), CH<sub>4</sub> concentrations (**b**), and dissolved oxygen (DO) with oxygen isopleths every 0.4 mg L<sup>-1</sup> (**c**). Anoxic water persisted at depth, and hypoxic water in the upper water suggests vertical mixing in

occurred. White dots on **b** mark sampling depths, white numbers indicate near-surface CH<sub>4</sub> concentrations, and red numbers indicates temperatures of isotherms

morning on day 240, when large methane diffusive fluxes

 ${\rm CH_4}$  ebullitive fluxes In the open water of both sites, ebullitive fluxes during low water were significantly higher than those during rising and high water (Kruskal–Wallis, p < 0.05), and higher or marginally higher than in the falling water periods (Kruskal–Wallis, p < 0.05 and p = 0.07, for embayment and open lake sites, respectively). For the flooded forest, no seasonal difference was found for the embayment site, while in the open lake, falling water ebullitve fluxes were higher than high water ones (Kruskal–Wallis, p < 0.05).

## Between habitat differences

Methane concentrations and fluxes differed between the open lake and embayment sites. Surface and bottom [CH<sub>4</sub>] were higher in most habitats of the embayment site, when compared to the same habitats in the open lake site (t-test, p < 0.01), with the exception of the macrophyte habitat, where no significant difference was found for bottom [CH<sub>4</sub>] (Mann–Whitney test, p = 0.14). Highest surface [CH<sub>4</sub>] concentration was measured in the macrophyte mats (95.6  $\mu$ M) (Table 1). A high surface [CH<sub>4</sub>] (15.5  $\mu$ M) was recorded for the open water habitat during May 2016, coinciding with the decay of macrophytes that grew during the exceptionally low water period in the previous year.

For diffusive fluxes, a significant difference was found only for the open water habitat, with higher fluxes at the embayment site (t-test, p = 0.0001, df = 92.5), while  $k_{617}$  values were higher in the open water (t test, p = 0.016, df = 91) and flooded forest (t test, p = 0.006, df = 43) habitats of the open lake site, compared to the same habitats at the embayment site. The highest diffusive flux was measured in the macrophyte mats during low water (2342  $\mu$ mol m<sup>-2</sup>



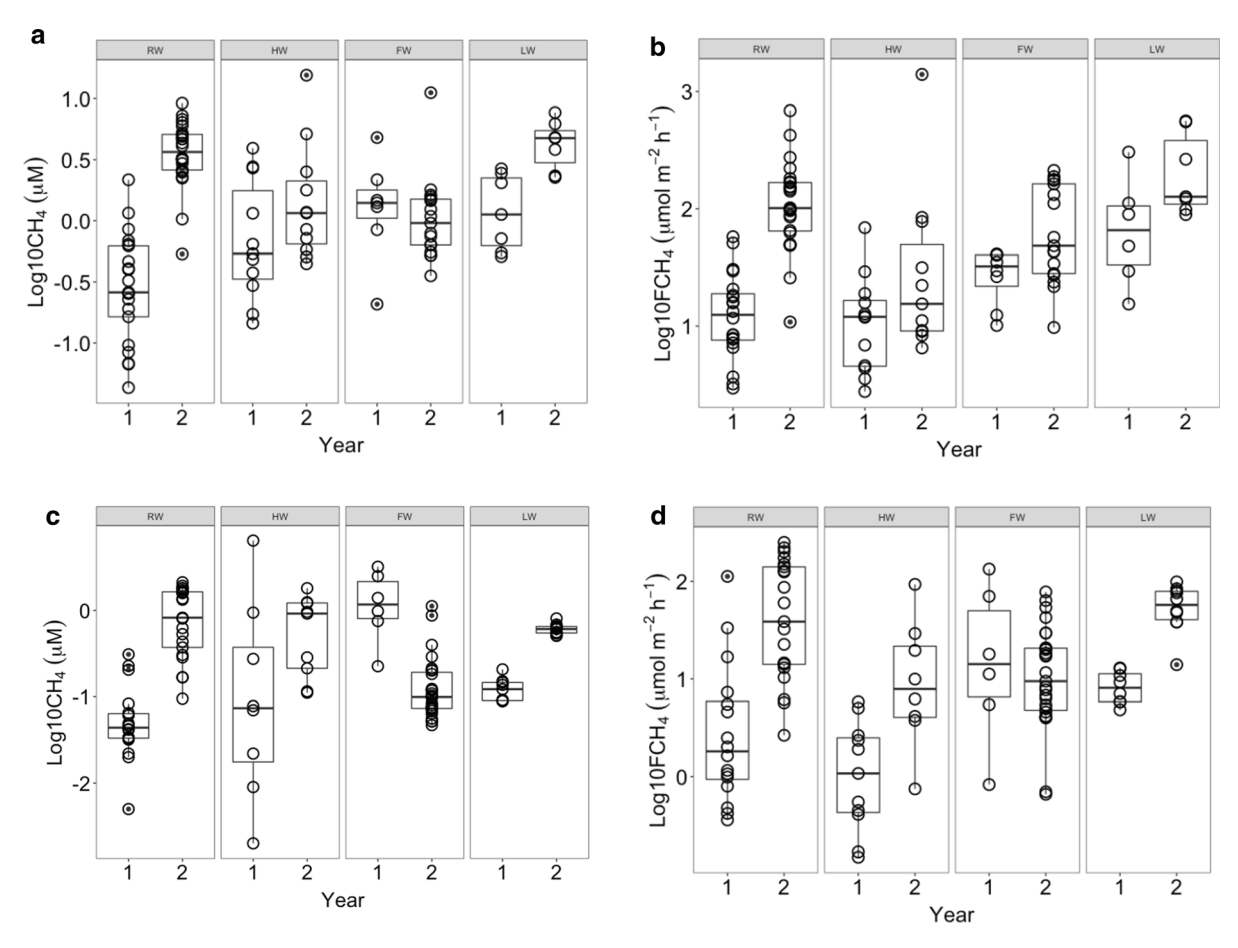


**Fig. 5** Comparison between CH<sub>4</sub> surface concentrations, and diffusive methane fluxes (FCH<sub>4</sub>) to the atmosphere, during rising (RW), high (HW), falling (FW), and low (LW) water periods, in two sampled hydrological years (named 1 and 2), for

open water habitats in the embayment  $(\mathbf{a}, \mathbf{b})$ , and open lake sites  $(\mathbf{c}, \mathbf{d})$ . Values are expressed in log-10. Boxes represent 25 and 75% quartiles, and lines the medians

h<sup>-1</sup>; Table 1) and coincided with the period of prolonged low water.

Surface and bottom [CH<sub>4</sub>] were significantly higher in the vegetated habitats, when all data are analyzed together (surface values, t-test, p < 0.0001; bottom values, Mann–Whitney test, p = 0.01; Fig. S4a). Diffusive and ebullitve fluxes did not differ between open water and vegetated habitats (19.6 and 14.5  $\mu$ mol m<sup>-2</sup> h<sup>-1</sup> for open water and vegetated habitats, respectively; t-test, p = 0.09; Fig. S4b).

## Interannual differences

Interannual comparisons for surface [CH<sub>4</sub>] were done only for the open water habitat and values measured during the rising and low water periods in year 2 were higher than the ones in year 1 for the embayment (Tukey post-test, p < 0.001; Fig. 5a), and open lake (Tukey post-test, p < 0.05; Fig. 5c) sites. Diffusive fluxes measured during the rising, high, and low water periods of year 2 were significantly higher than those measured in year 1 for the embayment (Tukey post-test, p < 0.0001; Fig. 5b), as well as for the open lake site (Tukey post-test, p < 0.0001; Fig. 5d).

# Day-night differences

Surface CH<sub>4</sub> concentrations, fluxes and  $k_{617}$  values were variable over the 24-h periods in all habitats for both sites. Values were higher during the day, but a significant difference between day and night was only found for diffusive fluxes (paired t-test, p = 0.0005,



df = 16) (Fig. 6) and  $k_{617}$  (paired t-test, p = 0.05, df = 16) in the open water habitat of the embayment site. This result is consistent with the day–night differences found for wind speed at this site, which were also significantly higher during the day (t-test, p < 0.0001).

The diel data were used to calculate daily  $CH_4$  diffusive fluxes for each habitat. We used the geometric mean of the diffusive fluxes made each day for each campaign, multiplied by 24, to estimate a daily  $CH_4$  diffusive flux and compared these values to the fluxes measured during mid-day (noon  $\pm$  3 h), multiplied by 24, as is commonly done in studies of  $CH_4$  emission. No statistical difference between the two ways of calculating daily values was observed for the open water and flooded forest habitats. For the macrophyte mats in the embayment site significantly higher daily values resulted when using measurements over 24 h periods (paired t-test, p = 0.006, df = 12); no significant difference was found at the open lake site.

Statistical relations between surface CH<sub>4</sub> concentrations and environmental variables

Using PCA analysis 11 variables were identified to include in a global model for open water (Fig. S5a), six variables for the macrophyte mats (Fig. S5b), and seven variables for the flooded forests (Fig. S5c). The top-ranked model for open water included the

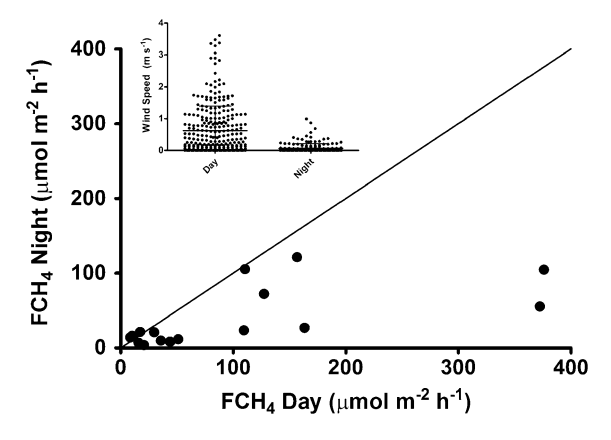


**Fig. 6** CH<sub>4</sub> diffusive fluxes (μmol m<sup>-2</sup> h<sup>-1</sup>) measured during the day versus those measured during the night for the open water habitat in the embayment. The line represents the 1:1 relation. The inset shows a comparison between day and night wind speeds (m s<sup>-1</sup>) in the same habitat. Horizontal lines represent mean and range; dots represent measurements

oxygenated portion of the water column (Z\_oxy), and surface water temperature and DO concentrations, and explained 39% (marginal R<sup>2</sup>) and 57% (conditional R<sup>2</sup>) of CH<sub>4</sub> concentration variability (Table 2). For the macrophyte mats, the top-ranked model included only the DO concentration at the bottom and maximum depth (zmax), explaining 29% (marginal R2) and 41% (conditional R2) of CH4 concentration variability (Table 2). The top-ranked model for flooded forest included bottom [CH<sub>4</sub>] and surface water temperature and explained around 65% of CH<sub>4</sub> concentration variability (Table 2). In addition to the variables included in the top-ranked models, TN and DOC were included in several of the selected models. All models with lower than 2 AICc units from the topranked models for each habitat are shown in Table 2. Information on the relation of the main variables selected for each habitat and their importance is shown in Table 3.

#### Discussion

Measurements of methane concentrations and fluxes in three representative habitats on the Amazon *várzea* indicate high diel, seasonal and interannual variability, with values spanning 3 to 4 orders of magnitude. Diel variability in fluxes and concentrations were as high as seasonal and interannual variability at both sites (Figs. 7, 8). We apply our results to evaluate the questions we posed.

How do environmental conditions during different hydrological phases influence methane concentrations and fluxes?

The best statistical models explaining differences in methane concentrations included DO concentrations in the surface and bottom waters, the oxygenated portion of the water column, water temperature, DOC and TN concentrations, and maximum depth. The statistical models revealed a negative relation between surface [CH<sub>4</sub>] and oxygenated part of the water column and surface DO, which is likely related to CH<sub>4</sub> oxidation by methanotrophs. Barbosa et al. (2018) have shown the importance of this biological process at L. Janauacá. Relationships with TN



Table 2 Summary of model averaged AICc weights, including all models within 2 AICc units of the top model for CH<sub>4</sub> surface water concentration for the open water, macrophyte and flooded forest habitats

Model variables	df	AICc	ΔΑΙС	wi	m-R <sup>2</sup>	c-R <sup>2</sup>
Open water						
Z_oxy, ntot, o2_s, temp_s	7	58.4	0.00	0.30	0.39	0.57
ntot, o2_s, temp_s, zmax	7	58.8	0.43	0.24	0.32	0.63
ntot, o2_s, temp_s, chla	7	59.1	0.77	0.21	0.34	0.60
ntot, o2_s, temp_s	6	60.1	1.76	0.13	0.27	0.53
ntot, o2_s, temp_s, o2_b	7	60.2	1.81	0.12	0.27	0.61
Macrophyte						
o2_b, zmax	5	37.5	0.00	0.51	0.29	0.41
o2_b, zmax, doc_b	6	37.6	0.04	0.50	0.38	0.45
Flooded forest						
ch4_b, temp_s	5	19.8	0.00	0.51	0.65	0.65
ch4_b, temp_s, ntot	6	21.0	1.26	0.26	0.64	0.69
ch4_b, temp_s, doc_s	6	21.2	1.43	0.24	0.64	0.69

All models include the random grouping factor for site. Degrees of freedom (df) in each model, small sample size corrected AIC (AICc), difference in AICc from top model ( $\Delta$ AIC), the AICc weight for a given model (wi), the marginal coefficient of determination estimates variance explained by fixed effects in a given model (m-R<sup>2</sup>), and the conditional R<sup>2</sup> is a measure of variance explained by both fixed and random effects (c-R<sup>2</sup>)

Z\_oxy oxygenated water column; ntot total dissolved nitrogen, o2\_s surface water DO concentration; surf\_s surface water temperature, zmax maximum depth, chla chlorophyll concentration; o2\_b bottom water DO concentration; doc\_b bottom water DOC concentration, ch4\_b bottom water CH<sub>4</sub> concentration, doc\_s surface water DOC concentration

**Table 3** Model full-averaged coefficients, standard errors (SE), z-tests (z) at p-values (p) for parameters included within final model sets for CH<sub>4</sub> surface concentration in the open water, macrophyte and flooded forest habitats

Variable	Estimate	SE	z	p	Relative importance
Open water					
(Intercept)	- 7.909	2.220	3.432	< 0.01	
Z_oxy	- 0.021	0.035	0.586	0.558	0.30
ntot	-0.324	0.121	2.586	< 0.001	1
o2_s	- 0.150	0.038	3.771	< 0.001	1
temp_s	0.302	0.074	3.925	< 0.001	1
zmax	- 0.011	0.023	0.496	0.620	0.24
chla	0.095	0.212	0.443	0.657	0.21
o2_b	0.008	0.027	0.318	0.750	0.12
Macrophyte					
(Intercept)	-0.001	0.083	0.013	0.99	
o2_b	-0.484	0.154	2.972	0.003	1
zmax	- 0.356	0.145	2.314	0.02	1
doc_b	0.138	0.173	0.777	0.437	0.5
Flooded forest					
(Intercept)	-0.0004	0.03	0.0	1	
ch4_b	0.20	0.7	3.3	0.0001	1
temp_s	0.15	0.7	4.7	0.01	1
ntot	0.02	0.7	0.5	0.6	0.26
doc_s	-0.03	0.9	0.5	0.7	0.24

Each coefficient is the weighted average, proportional to the Akaike weights for each model, across the subset of models which contained that variable. See the meaning of the symbols in Table 2



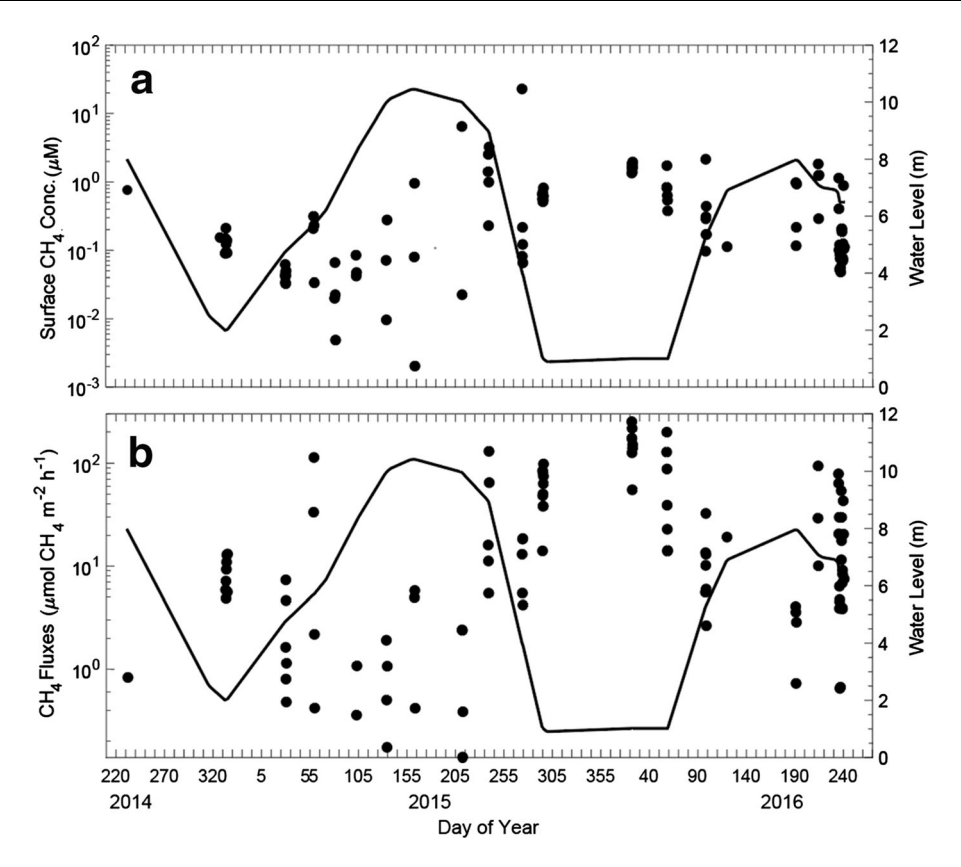


Fig. 7 Time series of methane  $(CH_4)$ , surface concentrations (a), and diffusive fluxes (b) for two hydrological years in the open water of the embayment. Black dots show the diel,

seasonal and interannual variations of those variables; black line shows changes in water level

concentrations have been associated with both oxidation and production of CH<sub>4</sub> in aquatic environments. Some studies have shown a positive correlation between CH<sub>4</sub> oxidation and nitrogen concentrations (Bender and Conrad 1995; Kruger et al. 2001), while others have found an opposite relation (Dunfield and Knowles 1995; Kightley et al. 1995). DOC is an important source of carbon and energy in aquatic systems (Wetzel 1990), and its quantity and quality have been shown to be related to CH<sub>4</sub> production (Bianchi et al. 1996; West et al. 2012). Consistent with that result, a positive relation between DOC and [CH<sub>4</sub>] occurred for the macrophyte habitat. Concentrations of DOC in bottom waters could be used as a proxy of organic matter availability for methanogenesis (Delsontro et al. 2011).

Previous work in Amazon floodplains has shown a dependency of vertical mixing on depth. According to MacIntyre and Melack (1984, 1988), when lakes are shallower than about 4 m, mixing to the bottom is

common by early morning. As lakes become deeper than 6 m, stratification tends to persist longer. In L. Janauacá, near-bottom CH<sub>4</sub> concentrations were higher during higher water levels for all habitats at the embayment site. During high water periods, vertical mixing was incomplete (e.g., Fig. 3), and CH<sub>4</sub> accumulated in the hypolimnion. In contrast, in the habitats of the open lake site complete mixing at night was more frequent. These differences in stratification and mixing contribute to differences in concentrations and diffusive fluxes found between the two sampling sites, though more analyses of mixing and turbulent processes are needed (e.g., MacIntyre et al. 2019).

How do CH<sub>4</sub> concentrations and fluxes to the atmosphere vary between day and night?

The present study is the first to our knowledge to show that day to night variations of surface dissolved CH<sub>4</sub>



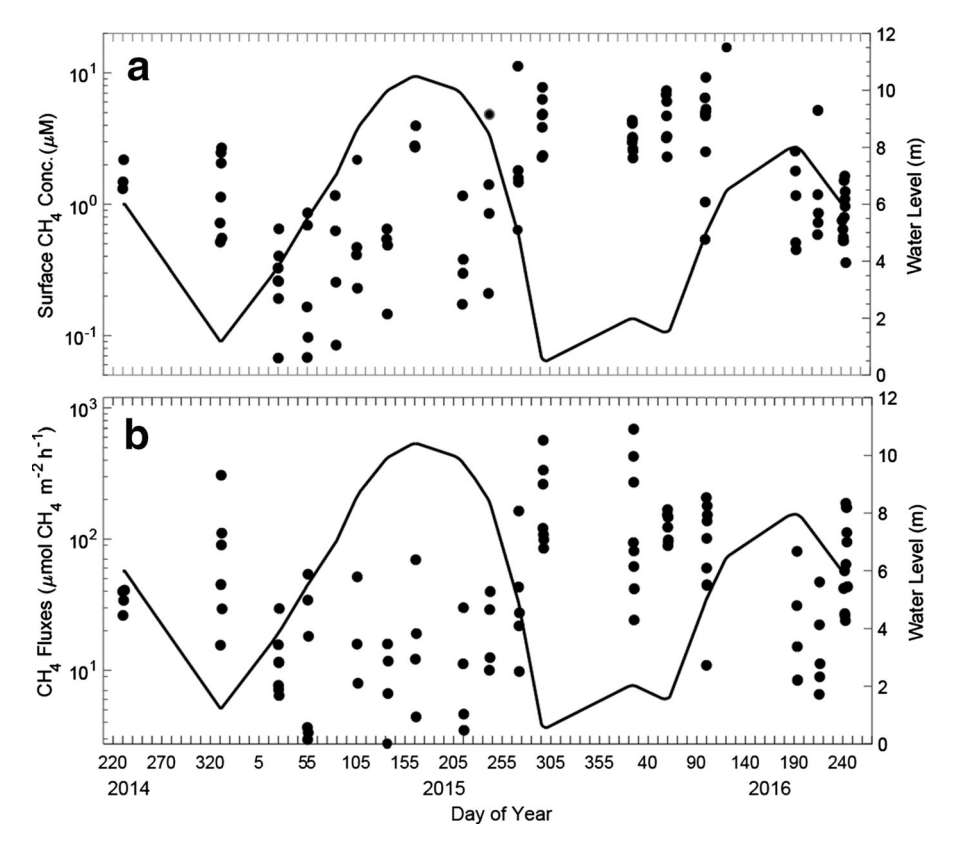


Fig. 8 Time series of methane  $(CH_4)$ , surface concentrations (a), and diffusive fluxes (b) for two hydrological years in the open water of the open lake site. Black dots show the diel,

seasonal and interannual variations of those variables; black line shows changes in water level

concentrations and fluxes to the atmosphere are of the same magnitude as seasonal variability on the Amazon floodplain. Variations of CH<sub>4</sub> flux over a day has been reported for other environments, and indicate higher fluxes during the day when compared to night for rice fields (Yun et al. 2013), fresh and salt-water marshes (Ding et al. 2004; Zhang and Ding 2011), and a lake in China (Xing et al. 2004). Our results from open water habitats are similar to these findings, and are probably related to day versus night differences in wind speeds (Fig. 6), which were significantly higher during the day than night. This is an interesting result that has important implications since the majority of measurements done in tropical lakes and wetlands have been made only during the daytime, which could overestimate daily fluxes. Though not statistically significant, fluxes in the macrophyte mats were higher during the night. This result contrasts with results from Käki et al. (2001) and Rõõm et al. (2014), who found higher fluxes during the day for CH<sub>4</sub> fluxes through aquatic

plants in boreal lakes, and pelagic and vegetated zones of a lake in Estonia, respectively.

Nocturnal mixing is often observed in tropical lakes (MacIntyre and Melack 1984, 1988; Tundisi et al. 1984). Such mixing occurred daily in L. Janauacá with Fig. 4 illustrating the deepening of the mixing layer as the water column was cooling ( $\sim$  day of year 239.7–240.3). Concurrently, water deficient in DO and richer in CH<sub>4</sub> was mixed to the surface such that surface concentrations increased from 1 to 3  $\mu$ M, and diffusive fluxes increased threefold.

Vertical and horizontal water movements are important in connecting the littoral, pelagic and benthic regions of lakes, and such movements could influence CH<sub>4</sub> dynamics on a diel basis (MacIntyre and Melack 1995). Patterns of stratification and mixing varied with fetch and proximity to the main river in a floodplain lake on the lower Amazon floodplain (Augusto-Silva et al. 2019). Where fetch was longer and the water deeper, the depth of mixing



was greater, as we found at the open lake site, supporting the inference of deeper diurnal thermoclines in places with greater exposure to wind. Augusto-Silva et al. (2019) also demonstrated that heat from upwind sites was transported downwind during windy periods. On relaxation of the wind, upwelling in the lower water column then induced near-surface water to flow back towards the original site. Hence, emissions from one site can be moderated by horizontal movements on diel time scales.

Lateral water movements did contribute to diel variation of CH<sub>4</sub> in L. Janauacá, with evidence suggesting exchange occurred between habitats. In the macrophyte mats, geometric mean CH<sub>4</sub> concentrations were approximately two times higher than in open water (Table 1). Even with higher CH<sub>4</sub> concentrations in the macrophyte mats, diffusive CH<sub>4</sub> fluxes were higher in the open water habitats. This difference implies that vegetated habitats, and particularly the macrophyte mats, act as sources of CH<sub>4</sub> to regions where conditions are more favorable for gas emission.

Biotic factors could also contribute to the diel variations observed in L. Janauacá. The consumption of CH<sub>4</sub> by microorganisms is known to influence both dissolved CH<sub>4</sub> concentrations and fluxes to the atmosphere (Bastviken 2009; Utsumi 1998a, b). In L. Janauacá, CH<sub>4</sub> oxidation consumes  $\sim 80\%$  of CH<sub>4</sub> from the water column in open water habitats during all hydrological periods (Barbosa et al. 2018). This process is dependent on DO and CH<sub>4</sub> concentrations (Bastviken et al. 2008; Utsumi et al. 1998a), which varied considerably during daytime in our sampled habitats and is inhibited by light (Dumestre et al. 1999). Oxidation may also be important in the vegetated habitats, especially in macrophyte mats (Laanbroek 2010; Ribaudo et al. 2017; Watson et al. 1997).

The large diel variability has implications for  $CH_4$  flux estimates. As shown by our results, daily  $CH_4$  flux estimates made using only values obtained during daytime periods (noon  $\pm$  3 h), as is commonly done by the majority of the published studies, can be different from daily estimates made using 24-h measurements. In macrophyte mats we found daily values were significantly higher when using 24-h measurements. It is possible that photosynthesis by periphyton, whose biomass per unit area can exceed that of phytoplankton (Engle and Melack 1993) in the mats during the day, as well as plant-transported DO (Chanton et al. 1992),

increased DO concentrations and, consequently oxidation of CH<sub>4</sub>.

Are fluxes higher in or near vegetated areas than in open waters?

Considerable spatial variability in CH<sub>4</sub> concentrations and fluxes to the atmosphere were observed in L. Janauacá. Although both surface and bottom CH<sub>4</sub> concentrations were higher in the vegetated habitats, no significant differences were found for either diffusive or ebullitive fluxes. Vegetated habitats have high rates of primary production (Melack and Forsberg 2001; Engle et al. 2008; Melack and Engle 2009), which may contribute to the elevated CH<sub>4</sub> concentrations by providing substrates for methanogenesis. However, organic carbon and dissolved CH<sub>4</sub> from these habitats can be advected to nearby open waters, as noted above.

Conditions for emission are less favorable in vegetated than in open water habitats, as seen by the lower  $k_{617}$  values in the vegetated habitats. MacIntyre et al. (2019) examined physical controls on gas transfer velocities in the flooded forest at our embayment site. They combined measurements of water-column temperature, meteorology and turbulence, calculated the rate of dissipation of turbulent kinetic energy, and used a surface renewal model to estimate k values, which were low and ranged from approximately 1 to 3 cm h<sup>-1</sup>.

How do extended periods of low water with associated growth and inundation of plants alter methane concentrations?

The significant interannual differnce in both dissolved CH<sub>4</sub> concentrations and fluxes to the atmosphere (Figs. 3, 4, 7, 8) is pertinent to the increasing occurrence of especially high and low water levels observed in the Amazon basin. The second sampled hydrological year had a prolonged low water period, as described in Amaral et al. (2018). The frequency of exceptional droughts and floods has increased in the last two decades in the Amazon region (Barichivich et al. 2018; Gloor et al. 2013), and is related to a combination of anthropogenic activities such as deforestation and changes in land-use, El-Niño and La-Niña effects, and anomalous heating of the North Atlantic sea surface, among other factors (Garcia et al.



2018). Exceptionally high water was reported in the central Amazon in 2012 and 2015, while severe droughts were reported during 2005 and 2010 (Marengo and Espinoza 2016). These hydrological conditions have important ecological consequences, such as increase in fire activity, tree mortality and emissions of carbon to the atmosphere (Duffy et al. 2015). The effects of exceptional floods on CO<sub>2</sub> emissions were discussed by Almeida et al. (2017) working in the Madeira River basin. During especially high water in 2014, CO<sub>2</sub> fluxes increased up to 50%.

We found that CH<sub>4</sub> surface concentrations and fluxes were considerably higher at both sites (embayment and open lake) following an especially low water period. Interannual differences were particularly high in the low and rising water periods of 2015 to 2016. During the extended low water period, Luziola spruceana and Oryza rufipogon covered large areas but senesced and decomposed when waters rose. The likely increase in labile organic matter could have increased methanogenesis resulting in elevated CH<sub>4</sub> concentrations and fluxes to the atmosphere as measured during the low and rising water periods of year 2, especially in habitats in the embayment. Amaral et al. (2018) present a temporal sequence of satellite images illustrating the coverage of the rooted herbaceous macrophytes and their loss as waters rose, and elevated pCO<sub>2</sub> values associated with the decay of the submerged plants. That the lake sediments dried during the prolonged drought and rewetted during the rising water period could also have contributed to the higher CH<sub>4</sub> fluxes measured in year 2. Increases in CH<sub>4</sub> concentrations and fluxes after the rewetting of sediments were found in Amazon lakes (Conrad et al. 2014) and tropical reservoirs (Kosten et al. 2018). According to Kannenberg et al. (2015), rewetted sediments can release nutrients due to disruption of soil aggregates and microbial lysis, which could stimulate microbial activity.

## Comparison to other studies

Few studies done in the Amazon have analyzed seasonal variability of  $CH_4$  concentrations and fluxes (Barbosa et al. 2016; Devol et al. 1990; Melack et al. 2004). Devol et al. (1990) found higher fluxes during high water. Our monthly sampling over two years indicated that both concentrations and fluxes tended to be higher when water levels were low with the

exception of flooded forest habitats, which had higher fluxes during falling water. This could be associated to less CH<sub>4</sub> oxidation in the water, as the water column was shallow, and the atmosphere and anoxic sediments were in closer proximity.

The fluxes reported here are similar to some and different from others measured in prior studies in the region (Table 4). To facilitate comparison, we report fluxes in mg CH<sub>4</sub> m<sup>-2</sup> d<sup>-1</sup>. Bartlett et al. (1988) used floating chambers and reported an arithmetic average diffusive flux for open water habitats of 8.3 mg CH<sub>4</sub> m<sup>-2</sup> d<sup>-1</sup>, which is considerably lower than our arithmetic average value when open water habitats of both sites are included (27.4 mg  $CH_4$  m<sup>-2</sup> d<sup>-1</sup>). Working in a várzea floodplain lake (L. Calado), Crill et al. (1988), using floating chambers, measured diffusive fluxes varying from 0 to 34 mg CH<sub>4</sub> m<sup>-2</sup> d<sup>-1</sup>, with an arithmetic average of 8.3 mg CH<sub>4</sub> m<sup>-2</sup> d<sup>-1</sup>. Bartlett et al. (1990) found considerably higher diffusive fluxes (mean value of 53 mg CH<sub>4</sub> m<sup>-2</sup> d<sup>-1</sup>) when working in open water environments during an exploratory survey along the Solimões River without habitats well characterized. Engle and Melack (2000) measured diffusive CH<sub>4</sub> fluxes ranging from 2 to 104 mg CH<sub>4</sub> m<sup>-2</sup> d<sup>-1</sup> (arithmetic average of 28 mg CH<sub>4</sub> m<sup>-2</sup> d<sup>-1</sup>), using floating chambers, while using the stagnant boundary layer approach they calculated values ranging from 0.9 to 50 mg CH<sub>4</sub> m<sup>-2</sup> d<sup>-1</sup>, with an arithmetic average of 11 mg CH<sub>4</sub> m<sup>-2</sup> d<sup>-1</sup>, in L. Calado. Engle and Melack (2000) reported diffusive flux one order of magnitude higher during a friagem (209 mg CH<sub>4</sub> m<sup>-2</sup> d<sup>-1</sup>), a large-scale cooling event (Caraballo et al. 2014). Barbosa et al. (2016) used floating chambers to estimate diffusive fluxes from 10 lakes in the central Amazon floodplain and reported values from below detection to 298 mg CH<sub>4</sub> m<sup>-2</sup> d<sup>-1</sup>, with overall arithmetic average of 59 mg CH<sub>4</sub> m<sup>-2</sup>

Information regarding  $CH_4$  fluxes in vegetated environments is scarce relative to open water environments, as is the number of limnological variables associated with  $CH_4$  dynamics, in previous studies (Table S3). Bartlett et al. (1988) reported a mean diffusive flux for flooded forest habitats of 50 mg  $CH_4$  m<sup>-2</sup> d<sup>-1</sup> (n = 66), which is more than five times higher than our mean diffusive flux of 4.3 mg  $CH_4$  m<sup>-2</sup> d<sup>-1</sup> (n = 158) for the same habitat. Their sampling was done mainly during daytime and on the edge of flooded forests with exposure to currents and winds,



**Table 4** Comparative table with information on sampled habitat, sampled season (L—low water, R—rising water, H—high water, F—falling water, W—wet, D—dry), CH<sub>4</sub> flux method (FC—floating chamber, D—discrete, C—continuous, S.F.M—stagnant film model, Fick method—estimate of FCH<sub>4</sub>

using water concentration and a chosen value of gas transfer velocity (k)), average diffusive flux rate (FCH<sub>4</sub>), and average CH<sub>4</sub> surface concentration ([CH<sub>4</sub>]) from the main studies included. When average value is not available range is shown

Habitat Regi	Region	Region Season	FCH <sub>4</sub> Method		FCH <sub>4</sub>	[CH <sub>4</sub> ]	References
			FC	Indirect	$(mg CH_4 m^{-2} d^{-1})$	$(\mu M)$	
Open water	Amazon	H/F	FC (D, C)	na	8.3	n.a	1
	Amazon	L	FC (D, C)	na	6 <sup>c</sup>	(0.1-5.5)	2
	Amazon	F	FC (D)	Fick	88 <sup>b</sup>	6.5	3
	Amazon	L, H <sup>c</sup>	FC (D)	Fick	44 <sup>b</sup>	3.7	4
	Amazon	L, R, H, F	FC (D, C)	na	4–10	n.a	5
	Amazon	R/H, L/F	FC (D)	Fick	28	0.25/2.9 <sup>a</sup>	6
	Amazon	L, R, H, F	FC (C)	na	27.4	1.5	7
	Pantanal	W, D	na	S.F.M	n.a	(0.08-1.1)	9
	Pantanal	D	FC (D)	na	5.4	n.a	10
	Orinoco	L, R, H, F	FC (D)	na	0.98	0.3	11
Macrophyte	Amazon	H/F	FC (D, C)	na	43.7	n.a	1
	Amazon	F	FC (D)	Fick	390 <sup>b</sup>	6.5	3
	Amazon	L, H <sup>a</sup>	FC (D)	Fick	214 <sup>b</sup>	9.7	4
	Amazon	L, R, H, F	FC (D, C)	na	35	n.a	5
	Amazon	L, R, H, F	FC (C)	na	55	5.7	7
	Amazon	H, F	FC (D)	na	158 <sup>b</sup>	n.a	8
	Pantanal	W, D	na	S.F.M	n.a	(0.8-76)	9
	Orinoco	L, R, H, F	FC (D)	na	0.75	0.3	11
Flooded forest	Amazon	H/F	FC (D, C)	na	50.5	n.a	1
	Amazon	F	FC (D)	Fick	75 <sup>b</sup>	6.5	3
	Amazon	L, H <sup>a</sup>	FC (D)	Fick	150 <sup>b</sup>	2.1	4
	Amazon	L, R, H, F	FC (D, C)	na	5.9	n.a	5
	Amazon	L, R, H, F	FC (C)	na	17.5	1.3	7
	Amazon	H, F	FC (D)	na	105 <sup>b</sup>	n.a	8
	Orinoco	L, R, H, F	FC (D)	na	2.5	0.3	11

FCH<sub>4</sub> and [CH<sub>4</sub>] columns: values inside parentheses represent range, while single values are averages, <sup>a</sup> represents values of L/H, <sup>b</sup> represents total flux, and <sup>c</sup> represents median values. 1—Bartlett et al. (1988), 2—Crill et al. (1988), 3—Devol et al. (1988), 4—Devol et al. (1990), 5—Wassmann et al. (1992), 6—Engle and Melack (2000), 7—present study, 8—Pangala et al. (2017), 9—Hamilton et al. (1995), 10—Peixoto et al. (2015), 11—Smith et al. (2000)

which could contribute to their higher mean value. Likewise, the mean value reported by Bartlett et al. (1990) (44 mg CH<sub>4</sub> m<sup>-2</sup> d<sup>-1</sup>, n = 58) for fringing flooded forests is also considerably higher than our mean value. Diffusive CH<sub>4</sub> fluxes from flooded forest measured by Wassmann et al. (1992) in a floodplain lake ranged from 1 to 12 mg CH<sub>4</sub> m<sup>-2</sup> d<sup>-1</sup>. Previous studies in floating macrophytes reported mean values similar to those measured in the present study (average

of 35.8 mg CH<sub>4</sub> m<sup>-2</sup> d<sup>-1</sup>). Bartlett et al. (1988, 1990) obtained average diffusive fluxes of 42 and 44 mg CH<sub>4</sub> m<sup>-2</sup> d<sup>-1</sup>, respectively, and Wassmann et al. (1992) reported values from 2 to 28 mg CH<sub>4</sub> m<sup>-2</sup> d<sup>-1</sup>.

 ${\rm CH_4}$  concentrations in vegetated habitats in other tropical floodplains, including the Pantanal (Hamilton et al. 1995, 2014; Peixoto et al. 2015), and the Orinoco (Smith et al. 2000) were considerably higher when compared to open water habitats. Hamilton et al.



(1995) sampled eight vegetated areas with similar herbaceous plant composition and environment characteristics as the macrophyte sites in L. Janauacá, and found dissolved CH<sub>4</sub> concentrations in these vegetated sites significantly higher than in open water sites. Peixoto et al. (2015) attributed the higher CH<sub>4</sub> fluxes found in the littoral vegetated area of a Pantanal floodplain lake to organic matter that can be used for methanogenesis.

Previous estimates of regional fluxes have been based on mean values; hence, our results have been expressed as means for comparison. Based on 212 chamber measurements and 149 bubble trap measurements made in the open water habitat, the most sampled habitat in the Amazon, we obtained a mean total flux of 85 mg  $CH_4$  m<sup>-2</sup> d<sup>-1</sup>, which is higher than the rate for open water habitat in Bartlett et al. (1988)  $(26 \text{ mg CH}_4 \text{ m}^{-2} \text{ d}^{-1}, \text{ n} = 22)$  and Melack et al. (2004) $(50 \pm 8 \text{ mg CH}_4 \text{ m}^{-2} \text{ d}^{-1}, \text{ n} = 66)$ . Based on 79 chamber measurements and 70 bubble trap measurements made in the flooded forest habitat, we obtained a mean of 110 mg  $CH_4\ m^{-2}\ d^{-1}$ , which is similar to the value of 121  $\pm$  53 mg CH<sub>4</sub> m<sup>-2</sup> d<sup>-1</sup> (n = 58) used Melack et al. (2004) for the flooded forest habitat. In the macrophyte habitat, based on 125 chamber measurements, we measured a mean diffusive CH<sub>4</sub> flux of 53 mg CH<sub>4</sub> m<sup>-2</sup> d<sup>-1</sup>. The diffusive rate in Bartlett et al. (1988) is similar (44 mg  $CH_4$  m<sup>-2</sup> d<sup>-1</sup>, n = 29). Though we did not use bubble traps in the macrophyte mats for logistic reasons, we can estimate ebullitive flux based on the percentage represented by this pathway to total flux in this habitat, estimated as 64% by Bartlett et al. (1988), and 67% by Wassmann et al. (1992). Using an average value of 65%, ebullitive flux for the macrophyte mats would be 97 mg CH<sub>4</sub> m<sup>-2</sup> d<sup>-1</sup>, totaling 150 mg CH<sub>4</sub> m<sup>-2</sup> d<sup>-1</sup>. Melack et al. (2004) used a high water value of 324  $\pm$  72 CH<sub>4</sub> m<sup>-2</sup>  $d^{-1}$  and a low water value of 121  $\pm$  33 CH<sub>4</sub> m<sup>-2</sup> d<sup>-1</sup> for their regional estimates.

#### Conclusion

The present study is the first to report dissolved CH<sub>4</sub> concentrations and fluxes at multiple spatial and temporal scales, together with anciliary limnological and meteorological data for the Amazon basin. Our results indicated large diel, seasonal and interannual variability in CH<sub>4</sub> concentrations and fluxes.

Environmental variables changed according to water level and affected CH<sub>4</sub> concentrations and fluxes. Though a clear seasonal trend was not observed, both concentrations and fluxes tended to be higher during low water periods. Stratification and mixing patterns, which differed among habitats, influenced CH<sub>4</sub> dynamics. Habitats at the open lake site, which experience higher winds, tended to mix to the bottom more frequently, oxygenating the water column, and creating less favorable conditions for CH<sub>4</sub> production and accumulation. Vegetated habitats have a major role in CH<sub>4</sub> dynamics in the Amazon, as seen by higher concentrations of the gas in this habitats, though fluxes are not different from those measured in open water regions. The interannual comparison in our study suggests that during prolonged periods of low water, the growth of macrophytes on exposed sediment, followed by the plant decomposition when water rises, could increase CH<sub>4</sub> concentrations and fluxes to the atmosphere. This has important implications as prolonged periods of especially low water are becoming more common in the Amazon basin. The results improve our knowledge of CH<sub>4</sub> dynamics in tropical floodplains and provide insight into environmental factors regulating fluxes to the atmosphere, with significant implication to regional and global CH<sub>4</sub> emission estimates.

Acknowledgements This work was supported by the Conselho Nacional de Pesquisa e Desenvolvimento-Ministério da Ciência Tecnologia (CNPq/MCTI); CNPq/LBA-Edital.68/2013, processo 458036/2013-7, CNPq-Universal processo.482004/2012-6. Post-graduate scholarships were provided to PMB and JHFA by Coordenação de Aperfeiçomento de Pessoal de Nível Superior (CAPES) and CNPq. PMB and JHFA are thankful to CAPES for the grant "Programa de Doutorado Sanduíche no Exterior  $-\ 88881.134945/2016\text{-}0100 \ \ \text{and} \ \ \text{``88881.135203/2016\text{-}0100}$ respectively. During manuscript preparation support was provided to PMB and JHFA by NASA Grant NNX17AK49G. JMM received support from National Aeronautics and Space Administration (NASA), the US Department of Energy (Contract No. DE-0010620), the US National Science Foundation (NSF DEB grant 1753856) and a Fulbright fellowship. VFF is partially supported by a CNPq productivity grant. The authors thank for the logistical support of INPA, João B. Rocha for the field support, and Lúcia Silva for offering a floating house as a research base. We thank Michaela Melo and Jonismar S. da Silva for help in field campaigns, and Nicholas Marino for assistance with statistical analyses.



#### References

- Almeida R, Pacheco FS, Barros N et al (2017) Extreme floods increase CO<sub>2</sub> outgassing from a large Amazonian river. Limnol Oceanogr 62:989–999. https://doi.org/10.1002/lno. 10480
- Amaral JHF, Borges AV, Melack JM et al (2018) Influence of plankton metabolism and mixing depth on CO<sub>2</sub> dynamics in an Amazon floodplain lake. Sci Total Environ 630:1381–1393. https://doi.org/10.1016/j.scitotenv.2018. 02.331
- Amaral JHF, Melack JM, Barbosa PM et al (2020) Carbon dioxide fluxes to the atmosphere from waters within flooded forests in the Amazon basin. J Geophys Res Biogeosciences. https://doi.org/10.1029/2019JG005293
- Augusto-Silva PB, MacIntyre S, de Moraes Rudorff C et al (2019) Stratification and mixing in large floodplain lakes along the lower Amazon River. J Great Lakes Res 45:61–72. https://doi.org/10.1016/j.jglr.2018.11.001
- Barbosa PM, Melack JM, Farjalla VF et al (2016) Diffusive methane fluxes from Negro, Solimões and Madeira rivers and fringing lakes in the Amazon basin. Limnol Oceanogr 61:S221–S237. https://doi.org/10.1002/lno.10358
- Barbosa PM, Farjalla VF, Melack JM et al (2018) High rates of methane oxidation in an Amazon floodplain lake. Biogeochemistry 137:351–365. https://doi.org/10.1007/s10533-018-0425-2
- Barichivich J, Gloor E, Peylin P et al (2018) Recent intensification of Amazon flooding extremes driven by strengthened Walker circulation. Sci Adv. https://doi.org/10.1126/ sciadv.aat8785
- Bartlett KB, Crill PM, Sebacher DI et al (1988) Methane flux from the central Amazonian floodplain. J Geophys Res 93:1571. https://doi.org/10.1029/JD093iD02p01571
- Bartlett KB, Crill PM, Bonassi J et al (1990) Methane flux from the Amazon River floodplain: emissions during rising water. J Geophys Res 95:16773–16788
- Barto'n K (2018) MuMIn: multi-model inference. R package version 1.42.1. https://CRAN.R-project.org/package=MuMIn. Accessed 25 Jan 2020
- Bastviken D (2009) Methane. In: Likens G (ed) Encyclopedia of inland waters, vol 1. Elsevier, Oxford, pp 783–805
- Bastviken D, Cole JJ, Pace ML, Van de Bogert MC (2008) Fates of methane from different lake habitats: connecting whole-lake budgets and CH<sub>4</sub> emissions. J Geophys Res Biogeosciences. https://doi.org/10.1029/2007JG000608
- Bates D, Maechler M, Bolker B et al (2017) lme4: fitting linear mixed-effects models using lme4. J Stat Softw 67:1–48. https://doi.org/10.18637/jss.v067.i01
- Bender M, Conrad R (1995) Effect of methane concentrations and soil conditions on the induction of methane oxidation activity. Soil Biol Biochem 27:1517–1527
- Bianchi TS, Freer ME, Wetzel RG (1996) Temporal and spatial variability, and the role of disolved organic carbon (DOC) in methane fluxes from the Sabine River Floodplain (Southeast Texas, U.S.A.). Arch Hydrobiol 136:261–287
- Bloom AA, Palmer PI, Fraser A, Reay DS (2012) Seasonal variability of tropical wetland CH<sub>4</sub> emissions: the role of the methanogen-available carbon pool. Biogeosciences 9:2821–2830. https://doi.org/10.5194/bg-9-2821-2012

- Bonnet MP, Pinel S, Garnier J et al (2017) Amazonian floodplain water balance based on modelling and analyses of hydrologic and electrical conductivity data. Hydrol Process 31(9):1702–1718. https://doi.org/10.1002/hyp.11138
- Bridgham SD, Cadillo-Quiroz H, Keller JK, Zhuang Q (2013) Methane emissions from wetlands: biogeochemical, microbial, and modeling perspectives from local to global scales. Glob Chang Biol 19:1325–1346. https://doi.org/10.1111/gcb.12131
- Caraballo P, Forsberg BR, Almeida F, Leite R (2014) Diel patterns of temperature, conductivity and dissolved oxygen in an Amazon floodplain lake: description of a friagem phenomenon. Acta Limnol Bras 26:318–331
- Chanton JP, Martens CS, Kelley CA et al (1992) Mechanisms and isotopic fractionation in emergent macrophytes of an Alaskan tundra lake. J Geophys Res 97:16681–16688
- Conrad R, Ji Y, Noll M et al (2014) Response of the methanogenic microbial communities in Amazonian oxbow lake sediments to desiccation stress. Environ Microbiol 16:1682–1694. https://doi.org/10.1111/1462-2920.12267
- Crill PM, Bartlett KB, Wilson JO et al (1988) Tropospheric methane from an Amazonian floodplain lake. J Geophys Res 93:1564–1570
- Delsontro T, Kunz MJ, Kempter T et al (2011) Spatial heterogeneity of methane ebullition in a large tropical reservoir. Environ Sci Technol 45:9866–9873. https://doi.org/10.1021/es2005545
- Devol AH, Richey JE, Clark WA et al (1988) Methane emissions to the troposphere from the Amazon floodplain. J Geophys Res 93:1583–1592
- Devol AH, Richey JE, Forsberg BR, Martinelli LA (1990) Seasonal dynamics in methane emissions from the Amazon River floodplain to the troposphere. J Geophys Res 95:417–426
- Ding W, Cai Z, Tsuruta H (2004) Diel variation in methane emissions from the stands of *Carex lasiocarpa* and *Deyeuxia angustifolia* in a cool temperate freshwater marsh. Atmos Environ 38(2):181–188. https://doi.org/10.1016/j.atmosenv.2003.09.066
- Duffy PB, Brando P, Asner GP, Field CB (2015) Projections of future meteorological drought and wet periods in the Amazon. Proc Natl Acad Sci 112:13172–13177. https:// doi.org/10.1073/pnas.1421010112
- Dumestre JF, Guézennec J, Galy-Lacaux C, Delmas R, Richard S, Labroue L (1999) Influence of light intensity on methanotrophic bacterial activity in Petit Saut Reservoir, French Guiana. Appl Environ Microbiol 65(2):534–539
- Dunfield P, Knowles R (1995) Kinetics of inhibition of methane oxidation by nitrate, nitrite, and ammonium in a humisol. Appl Environ Microbiol 61:3129–3135
- Engle D, Melack JM (1993) Consequences of riverine flooding for seston and the periphyton of floating meadows in an Amazon floodplain lake. Limnol Oceanogr 38:1500–1520
- Engle DL, Melack JM (2000) Methane emissions from an Amazon floodplain lake: enhanced release during episodic mixing and during falling water. Biogeochemistry 51:71–90
- Engle DL, Melack JM, Doyle RD, Fisher TR (2008) High rates of net primary productivity and turnover for floating grasses on the Amazon floodplain: implications for aquatic respiration and regional CO<sub>2</sub> flux. Glob Change Biol



- 14:369–381. https://doi.org/10.1111/j.1365-2486.2007.
- Garcia BN, Libonati R, Nunes A (2018) Extreme drought events over the Amazon basin: the perspective from the reconstruction of South American hydroclimate. Water 1:12–16
- Gelman A, Su Y-S (2018) arm: data analysis using regression and multilevel/hierarchical models. R package version 1.10-1. https://CRAN.R-project.org/package=arm. Accessed 20 Jan 2020
- Gloor M, Brienen RJW, Galbraith D et al (2013) Intensification of the Amazon hydrological cycle over the last two decades. Geophys Res Lett 40:1729–1733. https://doi.org/10.1002/grl.50377
- Grueber CE, Nakagawa S, Laws RJ, Jamieson IG (2011) Multimodel inference in ecology and evolution: challenges and solutions. J Evol Biol 24:699–711. https://doi.org/10.1111/j.1420-9101.2010.02210.x
- Gruner DS, Bracken MES, Berger SA et al (2017) Effects of experimental warming on biodiversity depend on ecosystem type and local species composition. Oikos 126:8–17. https://doi.org/10.1111/oik.03688
- Hamilton SK, Sippel SJ, Melack JM (1995) Oxygen depletion and carbon dioxide and methane production in waters of the Pantanal wetland of Brazil. Biogeochemistry 30:115–141. https://doi.org/10.1007/BF00002727
- Hamilton SK, Sippel SJ, Chanton JP, Melack JM (2014) Plant-mediated transport and isotopic composition of methane from shallow tropical wetlands. Inl Waters 4:369–376. https://doi.org/10.5268/IW-4.4.734
- Hess LL, Melack JM, Affonso AG et al (2015) Wetlands of the lowland amazon basin: extent, vegetative cover, and dualseason inundated area as mapped with JERS-1 synthetic aperture radar. Wetlands 35(4):745–756. https://doi.org/ 10.1007/s13157-015-0666-y
- Junk WJ (1997) The central Amazon floodplain. Springer, Berlin. https://doi.org/10.1007/978-3-662-03416-3
- Junk WJ, Piedade MTF, Schöngart J et al (2011) A classification of major naturally-occurring Amazonian lowland wetlands. Wetlands 31(4):623–640. https://doi.org/10.1007/ s13157-011-0190-7
- Kannenberg SA, Dunn ST, Ludwig SM et al (2015) Patterns of potential methanogenesis along soil moisture gradients following drying and rewetting in midwestern prairie pothole wetlands. Wetlands 35:633–640. https://doi.org/10. 1007/s13157-015-0653-3
- Kightley D, Nedwell DB, Cooper M (1995) Capacity for methane oxidation in landfill cover soils measured in laboratory-scale soil microcosms. Appl Environ Microbiol 61:592–601
- Kasper D, Amaral JHF, Forsberg BR (2018) The effect of filter type and porosity on total suspended sediment determinations. Anal Methods 10(46):5532–5539. https://doi.org/10. 1039/C8AY02134A
- Käki T, Ojala A, Kankaala P (2001) Diel variation in methane emissions from stands of *Phragmites australis* (cav.) trin. ex steud. and *Typha latifolia* L. in a boreal lake. Aquat Bot 71(4):259–271. https://doi.org/10.1016/S0304-3770(01)00186-3
- Kirschke S, Bousquet P, Ciais P et al (2013) Three decades of global methane sources and sinks. Nat Geosci 6:813–823. https://doi.org/10.1038/ngeo1955

- Kosten S, van den Berg S, Mendonça R et al (2018) Extreme drought boosts CO<sub>2</sub> and CH<sub>4</sub> emissions from reservoir drawdown areas. Inl Waters 0:1–12. https://doi.org/10. 1080/20442041.2018.1483126
- Kruger M, Frenzel P, Conrad R (2001) Microbial processes influencing methane emission from rice fields. Glob Chang Biol 7:49–63. https://doi.org/10.1046/j.1365-2486.2001.00395.x
- Laanbroek HJ (2010) Methane emission from natural wetlands: interplay between emergent macrophytes and soil microbial processes. A mini-review. Ann Bot 105:141–153. https://doi.org/10.1093/aob/mcp201
- MacIntyre S, Melack JM (1984) Vertical mixing in Amazon floodplain lakes. Verh Int Verein Limnol 22:1283–1287. https://doi.org/10.1080/03680770.1983.11897486
- MacIntyre S, Melack JM (1988) Frequency and depth of vertical mixing in an Amazon floodplain lake (L. Calado, Brazil). Verh Int Verein Limnol 23:80–85. https://doi.org/10.1080/03680770.1987.11897906
- MacIntyre S, Melack JM (1995) Vertical and horizontal transport in lakes: linking littoral, benthic, and pelagic habitats. J North Am Benthol Soc 14:599–615
- MacIntyre S, Jonsson A, Jansson M et al (2010) Buoyancy flux, turbulence, and the gas transfer coefficient in a stratified lake. Geophys Res Lett. https://doi.org/10.1029/2010GL044164
- MacIntyre S, Amaral JHF, Barbosa PM et al (2019) Turbulence and gas transfer velocities in sheltered flooded forests of the Amazon basin. Geophys Res Lett. https://doi.org/10. 1029/2019GL083948
- Marengo JA, Espinoza JC (2016) Extreme seasonal droughts and floods in Amazonia: causes, trends and impacts. Int J Climatol 36:1033–1050. https://doi.org/10.1002/joc.4420
- Melack JM, Forsberg BR (2001) Biogeochemistry of Amazon floodplain lakes and associated wetlands. In: McClain M, Victoria R, Richey J (eds) The bio-geochemistry of the Amazon Basin. Oxford University Press, Oxford, pp 235–274
- Melack JM, Engle D (2009) An organic carbon budget for an Amazon floodplain lake. Verh Int Verein Limnol 30:1179–1182. https://doi.org/10.1080/03680770.2009. 11923906
- Melack JM, Hess LL, Gastil M et al (2004) Regionalization of methane emissions in the Amazon Basin with microwave remote sensing. Glob Chang Biol 10:530–544. https://doi.org/10.1111/j.1529-8817.2003.00763.x
- Melton JR, Wania R, Hodson EL et al (2013) Present state of global wetland extent and wetland methane modelling: conclusions from a model inter-comparison project (WETCHIMP). Biogeosciences 10:753–788. https://doi.org/10.5194/bg-10-753-2013
- Nakagawa S, Schielzeth H (2013) A general and simple method for obtaining R<sup>2</sup> from generalized linear mixed-effects models. Methods Ecol Evol 4:133–142. https://doi.org/10.1111/j.2041-210x.2012.00261.x
- Oksanen J, Blanchet FG, Friendly M et al (2018) vegan: community ecology package. R package version 2.5-3. https:// CRAN.R-project.org/package=vegan
- Paiva RCD, Buarque DC, Collischonn W et al (2013) Largescale hydrologic and hydrodynamic modeling of the



- Amazon River basin. Water Resour Res 49(3):1226–1243. https://doi.org/10.1002/wrcr.20067
- Pangala SR, Enrich-Prast A, Basso LS et al (2017) Large emissions from floodplain trees close the Amazon methane budget. Nature 552:230–234. https://doi.org/10.1038/ nature24639
- Peixoto RB, Machado-Silva F, Marotta H et al (2015) Spatial versus day-to-day within-lake variability in tropical floodplain lake CH<sub>4</sub> emissions—developing optimized approaches to representative flux measurements. PLoS ONE 10:e0123319. https://doi.org/10.1371/journal.pone. 0123319
- Pinel S, Bonnet MP, Santos Da Silva J et al (2015) Correction of interferometric and vegetation biases in the SRTMGL1 spaceborne DEM with hydrological conditioning towards improved hydrodynamics modeling in the Amazon basin. Remote Sens 7:16108–16130. https://doi.org/10.3390/ rs71215822
- Poindexter CM, Baldocchi DD, Matthes JH et al (2016) The contribution of an overlooked transport process to a wetland's methane emissions. Geophys Res Lett 43:6276–6284. https://doi.org/10.1002/2016GL068782
- R Core Development Team (2018) R: a language and environment for statistical computing. https://www.R-project.org. Accessed 25 Jan 2020
- Ribaudo C, Bertrin V, Jan G et al (2017) Benthic production, respiration and methane oxidation in *Lobelia dortmanna* lawns. Hydrobiologia 784:21–34. https://doi.org/10.1007/s10750-016-2848-x
- Rõõm E-I, Nõges P, Feldmann T et al (2014) Years are not brothers: two-year comparison of greenhouse gas fluxes in large shallow Lake Võrtsjärv. Est J Hydrol 519:1594–1606. https://doi.org/10.1016/j.jhydrol.2014.09.
- Saunois M, Bousquet P, Poulter B et al (2016) The global methane budget: 2000–2012. Earth Syst Sci Data Discuss. https://doi.org/10.5194/essd-8-697-2016
- Smith L, Lewis W, Chanton JP (2000) Methane emissions from the Orinoco River floodplain, Venezuela. Biogeochemistry 51:113–140
- Strickland JDH, Parsons TR (1972) A practical handbook of seawater analysis. Fisheries Research Board of Canada. http://www.dfo-mpo.gc.ca/Library/1507.pdf
- Tedford EW, MacIntyre S, Miller SD, Czikowsky J (2014) Similarity scaling of turbulence in a temperate lake during fall cooling. J Geophys Res. https://doi.org/10.1002/ 2014JC010135
- Thottathil SD, Reis PCJ, Prairie YT (2019) Methane oxidation kinetics in northern freshwater lakes. Biogeochemistry. https://doi.org/10.1007/s10533-019-00552-x
- Tundisi JG, Forsberg BR, Devol AH et al (1984) Mixing patterns in Amazon lakes. Hydrobiologia 108:3–15. https://doi.org/10.1007/BF02391627
- Utsumi M, Nojiri Y, Nakamura T (1998a) Dynamics of dissolved methane and methane oxidation in dimictic Lake Nojiri during winter. Limnol Oceanogr 43:10–17

- Utsumi M, Nojiri Y, Nakamura T et al (1998b) Oxidation of dissolved methane in a eutrophic, shallow lake: Lake Kasumigaura, Japan. Limnol Oceanogr 43:471–480. doi:https://doi.org/10.4319/lo.1998.43.3.0471
- Valderrama JC (1981) The simultaneous analysis of total nitrogen and total phosphorus in natural waters. Mar Chem 10(2):109–122. https://doi.org/10.1016/0304-4203(81)90027-X
- Wang C, Xiao S, Li Y et al (2014) Methane formation and consumption processes in Xiangxi Bay of the three gorges reservoir. Sci Rep 4:1–7. https://doi.org/10.1038/ srep04449
- Wanninkhof R (2014) Relationship between wind speed and gas exchange over the ocean. Limnol Oceanogr Methods 12:351–362. https://doi.org/10.1029/92JC00188
- Wassmann R, Thein UG, Whiticar MJ et al (1992) Methane emissions from the Amazon floodplain: characterization of production and transport. Glob Biogeochem Cycles 6:3–13. https://doi.org/10.1029/91GB01767
- Watson A, Stephen KD, Nedwell DB, Arah JRM (1997) Oxidation of methane in peat: kinetics of  $CH_4$  and  $O_2$  removal and the role of plant roots. Soil Biol Biochem 29:1257–1267. https://doi.org/10.1016/S0038-0717(97)00016-3
- West WE, Coloso JJ, Jones SE (2012) Effects of algal and terrestrial carbon on methane production rates and methanogen community structure in a temperate lake sediment. Freshw Biol 57:949–955. https://doi.org/10.1111/j.1365-2427.2012.02755.x
- Wetzel RG (1990) Land-water interfaces: metabolic and limnological regulators. Verh Int Verein Limnol 24:6–24. https://doi.org/10.1080/03680770.1989.11898687
- Xing Y, Xie P, Yang H et al (2004) Diel variation of methane fluxes in summer in a eutrophic subtropical lake in China.

  J Freshw Ecol 19:639–644. https://doi.org/10.1080/02705060.2004.9664745
- Yamamoto S, Alcauskas JB, Crozier TE (1976) Solubility of methane in distilled water and seawater. J Chem Eng Data 21:78–80. https://doi.org/10.1021/je60068a029
- Yun S-I, Choi W-J, Choi J-E, Kim H-Y (2013) High-time resolution analysis of diel variation in methane emission from flooded rice fields. Commun Soil Sci Plant Anal 44:1620–1628. https://doi.org/10.1080/00103624.2012. 756510
- Zhang Y, Ding W (2011) Diel methane emissions in stands of *Spartina alterniflora* and *Suaeda salsa* from a coastal salt marsh. Aquat Bot 95:262–267. https://doi.org/10.1016/j.aquabot.2011.08.005
- **Publisher's Note** Springer Nature remains neutral with regard to jurisdictional claims in published maps and institutional affiliations.

